Manuel Stein

RESTRICTED

CLASSIFICATION CANCELLED

NATIONAL ADVISORY COMMITTEE FOR AERONAUTICS

TECHNICAL NOTE

No. 962

ANALYSIS OF SQUARE SHEAR WEB ABOVE BUCKLING LOAD

By Samuel Levy, Kenneth L. Fienup, and Ruth M. Woolley
National Bureau of Standards

Washington
February 1945

CLASSIFIED DOCUMENT

This document contains classified information affecting the National Defense of the United States within the meaning of the Espionage Act, USC 50:31 and 32. Its transmission or the revelation of its contents in any manner to an unauthorized person is prohibited by law. Information so classified may be imparted only to persons in the military and naval Services of the United States, appropriate civilian officers and employees of the Federal Government who have a legitimate interest therein, and to United States citizens of known loyalty and discretion who of necessity must be informed thereof.

RESTRICTED

CLASSIFICATION CANCELLED

NATIONAL ADVISORY COMMITTEE FOR AERONAUTICS

TECHNICAL NOTE NO. 962

ANALYSIS OF SQUARE SHEAR WEB ABOVE BUCKLING LOAD

By Samuel Levy, Kenneth L. Fienup, and Ruth M. Woolley

SUMMARY

A solution of Von Karman's fundamental equations for plates with large deflections is presented for the case of a shear web divided into square panels by reinforcing struts. Numerical solutions are given for struts of infinite rigidity and for struts the weight of which is one-fourth the weight of the sheet. The results are compared with Wagner's diagonal tension theory as extended by Kuhn and by Langhaar. It is found that the diagonal tension theory as developed by Kuhn agrees best with the present paper in the practical range when $r = 1/4$. Kuhn's theory is in especially good agreement for the force in the strut when $r = 1/4$.

INTRODUCTION

The necessity for designing structures having the smallest possible weight for a given load has forced airplane designers to build wing-beams and monocoque boxes with shear webs so thin that they may be buckled in a diagonal direction under service loads. As the shear load is increased well above the buckling load, it is carried principally by diagonal tension along the buckles. The beam approaches a "diagonal-tension field" beam.

The load at which such shear webs will buckle has been determined by several authors. (See, for example, pp. 357 to 363 of reference 1.) After buckling, the behavior of the web is frequently determined from Wagner's diagonal-tension-field theory (references 2 and 3) which neglects the flexural rigidity of the sheet. Experimental results (see p. 2 of reference 4, pp. 18 and 19 of reference 5, and p. 5 of reference 6) indicate that Wagner's diagonal-tension-

field theory may be too conservative for constructions in which the diagonal tension field is only partially developed.

An analysis of the behavior of a flat plate subjected to shearing loads covering the range from the start of buckling to the development of a full diagonal tension field was, therefore, thought desirable. Such an analysis, based on Von Kármán's large deflection equations, was made for the case of a shear web divided into square panels by vertical struts.

This investigation, conducted at the National Bureau of Standards, was sponsored by and conducted with the financial assistance of the National Advisory Committee for Aeronautics.

SYMBOLS

The following symbols are used (see also fig. 1):

a plate length and plate width

h plate thickness

w normal displacement of points of the middle surface

E Young's modulus

μ Poisson's ratio, assumed to be $\sqrt{0.1} = 0.316$

x,y coordinate axes with origin at corner of one bay of the web plate

$D = \frac{Eh^3}{12(1-\mu^2)} = \frac{Eh^3}{10.8}$ flexural rigidity of the plate

F stress function

Q shear load carried by beam

$\bar{\sigma}_x$ average stress in plate in x-direction

$\bar{\sigma}_y$ average stress in plate in y-direction

τ shear stress at corners of plate

r ratio of strut area to plate area

P compressive force in strut

ϵ_x', ϵ_y', γ_{xy}'	median fiber strains
σ_x', σ_y', τ_{xy}'	median fiber stresses
σ_x'', σ_y'', τ_{xy}''	extreme fiber bending stresses
A_m, B_n	coefficients in stress function
p	lateral pressure
$b_{m,n}$	coefficient in stress function
$w_{m,n}$	coefficient in deflection function
m, n	integral numbers used as subscripts
$\bar{\gamma} = 2.632\tau/E$	apparent shearing deformation of beam ($\bar{\gamma}$ is the angle through which the flanges of the beam rotate relative to the struts)
u,v	displacements in x and y directions, respectively,
M	bending moment in flange

FUNDAMENTAL EQUATIONS

Consider an initially flat square plate of uniform thickness. Two opposite edges are assumed to be simply supported by heavy flanges, integral with the plate, which allow rotation about the edges but prevent displacement parallel to the edges and force the edges to remain straight. The other two edges are simply supported by struts, integral with the plate, which allow rotation about the eges and displacement parallel to the edges corresponding to shortening of the strut under load but maintain the edges in a straight line.

EQUATIONS FOR THE DEFORMATIONS OF THIN PLATES

The fundamental equations governing the deformation of thin plates were developed by Von Karman. They are (see reference 1, pp. 322-323):

$$\frac{\partial^4 F}{\partial x^4} + 2\frac{\partial^4 F}{\partial x^2 \partial y^2} + \frac{\partial^4 F}{\partial y^4} = E\left[\left(\frac{\partial^2 w}{\partial x \partial y}\right)^2 - \frac{\partial^2 w}{\partial x^2}\frac{\partial^2 w}{\partial y^2}\right] \tag{1}$$

$$\frac{\partial^4 w}{\partial x^4} + 2\frac{\partial^4 w}{\partial x^2 \partial y^2} + \frac{\partial^4 w}{\partial y^4} = \frac{p}{D} + \frac{h}{D}\left(\frac{\partial^2 F}{\partial y^2}\frac{\partial^2 w}{\partial x^2} + \frac{\partial^2 F}{\partial x^2}\frac{\partial^2 w}{\partial y^2} - 2\frac{\partial^2 F}{\partial x \partial y}\frac{\partial^2 w}{\partial x \partial y}\right) \tag{2}$$

where the median-fiber stresses are

$$\sigma_x' = \frac{\partial^2 F}{\partial y^2}, \quad \sigma_y' = \frac{\partial^2 F}{\partial x^2}, \quad \tau_{xy}' = -\frac{\partial^2 F}{\partial x \partial y} \tag{3}$$

and the median-fiber strains are

$$\left.\begin{aligned} \epsilon_x' &= \frac{1}{E}\left(\frac{\partial^2 F}{\partial y^2} - \mu\frac{\partial^2 F}{\partial x^2}\right) \\ \epsilon_y' &= \frac{1}{E}\left(\frac{\partial^2 F}{\partial x^2} - \mu\frac{\partial^2 F}{\partial y^2}\right) \\ \gamma_{x,y}' &= -\frac{2(1+\mu)}{E}\frac{\partial^2 F}{\partial x \partial y} \end{aligned}\right\} \tag{4}$$

The extreme-fiber bending stresses are

$$\left.\begin{aligned} \sigma_x'' &= -\frac{Eh}{2(1-\mu^2)}\left(\frac{\partial^2 w}{\partial x^2} + \mu\frac{\partial^2 w}{\partial y^2}\right) \\ \sigma_y'' &= -\frac{Eh}{2(1-\mu^2)}\left(\frac{\partial^2 w}{\partial y^2} + \mu\frac{\partial^2 w}{\partial x^2}\right) \\ \tau_{x,y}'' &= -\frac{Eh}{2(1+\mu)}\frac{\partial^2 w}{\partial x \partial y} \end{aligned}\right\} \tag{5}$$

EQUILIBRIUM OF MEDIAN FIBER FORCES

Seydel (reference 7, p. 181) showed that the buckling load of a simply supported square plate subjected to shearing forces is given with an error of less than 1 percent if the deflection is described by

$$w = w_{1,1} \sin \frac{\pi x}{a} \sin \frac{\pi y}{a} + w_{1,3} \sin \frac{\pi x}{a} \sin \frac{3\pi y}{a}$$

$$+ w_{3,1} \sin \frac{3\pi x}{a} \sin \frac{\pi y}{a} + w_{2,2} \sin \frac{2\pi x}{a} \sin \frac{2\pi y}{a}$$

$$+ w_{3,3} \sin \frac{3\pi x}{a} \sin \frac{3\pi y}{a} \qquad (6)$$

where $w_{1,1}$, $w_{1,3}$, $w_{3,1}$, $w_{2,2}$, and $w_{3,3}$ are five adjustable constants. The analysis will be carried well beyond the buckling load on the assumption that expression (6) continues to give an adequate description of the buckles in the plate.

A suitable stress function F must now be chosen to satisfy equation (1) which expresses the condition that the median fiber forces are in equilibrium in the plane of the web. If F is taken as,

$$F = \frac{\bar{\sigma}_x y^2}{2} + \frac{\bar{\sigma}_y x^2}{2} - \tau xy + \sum_{m=0}^{6} \sum_{n=0}^{6} b_{m,n} \cos \frac{m\pi x}{a} \cos \frac{n\pi y}{a}$$

$$+ \sum_{m=2,4,6} A_m \cos \frac{m\pi x}{a} \left[\left(\frac{1-\mu}{1+\mu} - \frac{m\pi}{2} \coth \frac{m\pi}{2}\right) \cosh m\pi \left(\frac{y}{a} - \frac{1}{2}\right)\right.$$

$$\left. + m\pi \left(\frac{y}{a} - \frac{1}{2}\right) \sinh m\pi \left(\frac{y}{a} - \frac{1}{2}\right)\right]$$

$$+ \sum_{m=1,3,5} A_m \cos \frac{m\pi x}{a} \left[\left(\frac{1-\mu}{1+\mu} - \frac{m\pi}{2} \tanh \frac{m\pi}{2}\right) \sinh m\pi \left(\frac{y}{a} - \frac{1}{2}\right)\right.$$

$$\left. + m\pi \left(\frac{y}{a} - \frac{1}{2}\right) \cosh m\pi \left(\frac{y}{a} - \frac{1}{2}\right)\right]$$

$$+ \sum_{n=2,4,6} B_n \cos \frac{n\pi y}{a} \left[\left(\frac{1-\mu}{1+\mu} - \frac{n\pi}{2} \coth \frac{n\pi}{2}\right) \cosh n\pi \left(\frac{x}{a} - \frac{1}{2}\right)\right.$$

$$\left. + n\pi \left(\frac{x}{a} - \frac{1}{2}\right) \sinh n\pi \left(\frac{x}{a} - \frac{1}{2}\right)\right]$$

$$+ \sum_{n=1,3,5} B_n \cos \frac{n\pi y}{a} \left[\left(\frac{1-\mu}{1+\mu} - \frac{n\pi}{2} \tanh \frac{n\pi}{2}\right) \sinh n\pi \left(\frac{x}{a} - \frac{1}{2}\right)\right.$$

$$\left. + n\pi \left(\frac{x}{a} - \frac{1}{2}\right) \cosh n\pi \left(\frac{x}{a} - \frac{1}{2}\right)\right] \quad (7)$$

and if equations (6) and (7) are substituted into equation (1) it is found by a method shown in reference 8 that equation (1) is identically satisfied when

$$
\left.
\begin{aligned}
b_{0,0} &= 0 \\
b_{0,2} &= \frac{E}{64}(2w_{1,1}^2 - 4w_{1,1}w_{1,3} + 18w_{3,1}^2 - 36w_{3,1}w_{3,3}) \\
b_{0,4} &= \frac{E}{1024}(16w_{1,1}w_{1,3} + 144w_{3,1}w_{3,3} + 32w_{2,2}^2) \\
b_{0,6} &= \frac{E}{5184}(162w_{3,3}^2 + 18w_{1,3}^2) \\
b_{1,1} &= \frac{E}{16}(-16w_{2,2}w_{1,3} - 16w_{2,2}w_{3,1}) \\
b_{1,3} &= \frac{E}{400}(16w_{1,1}w_{2,2} + 64w_{2,2}w_{3,1}) \\
b_{1,5} &= \frac{E}{2704}(64w_{2,2}w_{1,3} + 144w_{2,2}w_{3,3}) \\
b_{2,0} &= \frac{E}{64}(2w_{1,1}^2 - 4w_{1,1}w_{3,1} - 36w_{1,3}w_{3,3} + 18w_{1,3}^2) \\
b_{2,2} &= \frac{E}{256}(16w_{1,1}w_{3,1} + 16w_{1,1}w_{1,3} - 64w_{1,3}w_{3,1}) \\
b_{2,4} &= \frac{E}{1600}(100w_{1,3}w_{3,1} - 4w_{1,1}w_{1,3} + 36w_{1,1}w_{3,3}) \\
b_{2,6} &= \frac{E}{6400}(144w_{1,3}w_{3,3}) \\
b_{3,1} &= \frac{E}{400}(16w_{1,1}w_{2,2} + 64w_{1,3}w_{2,2}) \\
b_{3,3} &= 0 \\
b_{3,5} &= \frac{E}{4624}(-16w_{1,3}w_{2,2}) \\
b_{4,0} &= \frac{E}{1024}(32w_{2,2}^2 + 16w_{1,1}w_{3,1} + 144w_{3,3}w_{1,3}) \\
b_{4,2} &= \frac{E}{1600}(100w_{1,3}w_{3,1} - 4w_{1,1}w_{3,1} + 36w_{1,1}w_{3,3}) \\
b_{4,4} &= \frac{E}{4096}(-64w_{1,3}w_{3,1}) \\
b_{4,6} &= \frac{E}{10816}(-36w_{1,3}w_{3,3}) \\
b_{5,1} &= \frac{E}{2704}(64w_{2,2}w_{3,1} + 144w_{2,2}w_{3,3}) \\
b_{5,3} &= \frac{E}{4624}(-16w_{3,1}w_{2,2}) \\
b_{5,5} &= 0 \\
b_{6,0} &= \frac{E}{5184}(162w_{3,3}^2 + 18w_{3,1}^2) \\
b_{6,2} &= \frac{E}{6400}(144w_{3,1}w_{3,3}) \\
b_{6,4} &= \frac{E}{10816}(-36w_{3,1}w_{3,3}) \\
b_{6,6} &= 0 \\
b_{m,n} &= 0 \quad \text{whenever} \quad m+n \quad \text{is an odd number}
\end{aligned}
\right\} \quad (8)
$$

BOUNDARY CONDITIONS

The condition that the edges of the plate be simply supported is automatically satisfied by equation (6) for the lateral deflection.

The condition that the edges of the plate act integrally with the supporting struts and flanges of the beam requires that the strain at the edge of the plate be equal to the strain in the supporting strut or flange. This condition will be used to determine the remaining coefficients $\bar{\sigma}_x$, $\bar{\sigma}_y$, A_m, and B_n in equation (7).

The edges $y = 0$, $y = a$ (see fig. 1) are considered to be supported by flanges so heavy that they do not shorten under load. The median fiber strain in the x-direction at the edges $y = 0$, $y = a$ must, therefore, be zero.

$$(\epsilon_x')_{y=o,y=a} = 0 \tag{9}$$

The edges $x = o$ and $x = a$ are considered to be supported by struts having a cross-sectional area of $r\,a\,h$. Such struts will shorten under load. If the compressive force in the strut is denoted by P, the median fiber strain in the y-direction at the edges $x = o$, $x = a$ must be

$$(\epsilon_y')_{x=o,x=a} = -\frac{P}{rahE} \tag{10}$$

Since there are an equal number of web bays and struts, the compressive force in a strut must equal the vertical tensile force in a web bay, or

$$P = \int_o^a (h\sigma_y')\,dx \tag{11}$$

Substituting from equations (3) and (7) into equation (11) and performing the indicated integration gives,

$$P = ah\bar{\sigma}_y + \frac{4h}{(1+\mu)a} \sum_{n=2,4,6} n\pi B_n \sinh \frac{n\pi}{2} \cos \frac{n\pi y}{a} \quad (12)$$

Substituting equation (12) into equation (10) gives

$$(\epsilon_y')_{x=0,\,x=a} = -\frac{\bar{\sigma}_y}{rE} - \frac{4\pi}{(1+\mu)ra^2E} \sum_{n=2,4,6} nB_n \sinh \frac{n\pi}{2} \cos \frac{n\pi y}{a} \quad (13)$$

The fact that the summations in the series expansion for F equation (7) have been limited to m and n = 6 makes it impossible to satisfy identically the boundary equations (9) and (13). Except for a small variation in strain of a frequency higher than the sixth harmonic, however, it can be shown by expanding F into trigonometric series and by substituting equations (4), (7), and (8) into equations (9) and (13) that equations (9) and (13) are satisfied

for $r = \infty$ $(w_{1,3} = w_{3,1})$, when

$$\left.\begin{aligned}
\bar{\sigma}_y=\bar{\sigma}_x&=\frac{E}{a^2}\left(1.804w_{1,1}^2+18.04w_{1,3}^2+16.24w_{3,3}^2+7.217w_{2,2}^2\right)\\
A_1=B_1&=\frac{E}{10^2}\left(-7.079w_{1,1}w_{2,2}-12.09w_{1,3}w_{2,2}-26.96w_{3,3}w_{2,2}\right)\\
A_2=B_2&=\frac{E}{10^3}\left(-0.3838w_{1,1}^2-1.295w_{1,3}^2-0.0775w_{3,3}^2-0.0856w_{2,2}^2\right.\\
&\qquad\left.+3.693w_{1,1}w_{1,3}+3.207w_{1,1}w_{3,3}+14.04w_{1,3}w_{3,3}\right)\\
A_3=B_3&=\frac{E}{10^4}\left(+0.159w_{1,1}w_{2,2}+2.397w_{1,3}w_{2,2}-1.581w_{3,3}w_{2,2}\right)\\
A_4=B_4&=\frac{E}{10^5}\left(-0.0463w_{1,1}^2-2.414w_{1,3}^2-0.1666w_{3,3}^2-1.506w_{2,2}^2\right.\\
&\qquad\left.-0.278w_{1,1}w_{1,3}+0.162w_{1,1}w_{3,3}-6.10w_{1,3}w_{3,3}\right)\\
A_5=B_5&=\frac{E}{10^6}\left(-0.2504w_{1,1}w_{2,2}+1.920w_{1,3}w_{2,2}+3.289w_{3,3}w_{2,2}\right)\\
A_6=B_6&=\frac{E}{10^7}\left(-0.0535w_{1,1}^2-1.181w_{1,3}^2-6.30w_{3,3}^2-.214w_{2,2}^2\right.\\
&\qquad\left.+0.417w_{1,1}w_{1,3}+0.417w_{1,1}w_{3,3}-2.297w_{1,3}w_{3,3}\right)
\end{aligned}\right\}\quad(14a)$$

and for $r = 0.25$, when

$$\bar{\sigma}_x = \frac{E}{a^2}(+1.338w_{1,1}^2 + 1.975w_{1,3}^2 + 11.41w_{3,1}^2 + 5.354w_{2,2}^2 + 13.[illegible]w_{3,3}^2)$$

$$\bar{\sigma}_y = \frac{E}{a^2}(+0.3313w_{1,1}^2 + 3.348w_{1,3}^2 + 0.3378w_{3,1}^2 + 1.335w_{2,2}^2 + 3.382w_{3,3}^2)$$

$$A_1 = \frac{E}{10^2}(-7.079w_{1,1}w_{2,2} - 1.679w_{1,3}w_{2,2} - 10.42w_{3,1}w_{2,2} - 26.38w_{3,2}w_{3,3})$$

$$B_1 = \frac{E}{10^2}(-7.079w_{1,1}w_{2,2} - 10.42w_{1,3}w_{2,2} - 1.679w_{3,1}w_{2,2} - 38.98w_{2,2}w_{3,3})$$

$$A_2 = \frac{E}{10^4}(-3.572w_{1,1}^2 - 29.50w_{1,3}^2 - 3.713w_{3,1}^2 - 0.3007w_{2,2}^2 - 0.3823w_{3,3}^2$$
$$+ 12.79w_{1,1}w_{1,3} + 31.68w_{1,1}w_{3,1} + 122.78w_{1,3}w_{3,3} + 3.743w_{3,1}w_{3,3}$$
$$+ 20.46w_{1,3}w_{3,1} + 29.87w_{1,1}w_{3,3})$$

$$B_2 = \frac{E}{10^4}(-3.135w_{1,1}^2 - 3.703w_{1,3}^2 - 17.07w_{3,1}^2 - 0.4593w_{2,2}^2 - 0.4184w_{3,3}^2$$
$$+ 12.97w_{1,1}w_{1,3} + 3.147w_{1,1}w_{3,1} + 3.295w_{1,3}w_{3,3} + 70.34w_{3,1}w_{3,3}$$
$$+ 12.42w_{1,3}w_{3,1} + 19.32w_{1,1}w_{3,3})$$

$$A_3 = \frac{E}{10^4}(+0.1590w_{1,1}w_{2,2} + 3.258w_{1,3}w_{2,2} + 0.1333w_{3,1}w_{2,2} - 1.578w_{2,2}w_{3,3})$$

$$B_3 = \frac{E}{10^4}(+0.1590w_{1,1}w_{2,2} + 0.1333w_{1,3}w_{2,2} + 3.258w_{3,1}w_{2,2} - 1.578w_{2,2}w_{3,3})$$

$$A_4 = \frac{E}{10^5}(-0.02885w_{1,1}^2 - 0.03677w_{1,3}^2 - 0.1834w_{3,1}^2 - 1.469w_{2,2}^2 - 0.1307w_{3,3}^2$$
$$+ 0.1133w_{1,1}w_{1,3} - 0.5821w_{1,1}w_{3,1} - 6.982w_{1,3}w_{3,3} + 0.3615w_{3,1}w_{3,3}$$
$$- 3.042w_{1,3}w_{3,1} + 0.00478w_{1,1}w_{3,3})$$

$$B_4 = \frac{E}{10^5}(-0.03034w_{1,1}^2 - 0.2381w_{1,3}^2 - 0.04708w_{3,1}^2 - 1.101w_{2,2}^2 - 0.1177w_{3,3}^2$$
$$- 0.3786w_{1,1}w_{1,3} + 0.1414w_{1,1}w_{3,1} + 0.5727w_{1,3}w_{3,3} - 5.181w_{3,1}w_{3,3}$$
$$- 1.470w_{1,3}w_{3,1} + 0.08832w_{1,1}w_{3,3})$$

$$A_5 = \frac{E}{10^6}(-0.2504w_{1,1}w_{2,2} - 0.2245w_{1,3}w_{2,2} + 2.143w_{3,1}w_{2,2} + 3.285w_{2,2}w_{3,3})$$

$$B_5 = \frac{E}{10^6}(-0.2504w_{1,1}w_{2,2} + 2.143w_{1,3}w_{2,2} - 0.2245w_{3,1}w_{2,2} + 3.285w_{2,2}w_{3,3})$$

$$A_6 = \frac{E}{10^7}(-0.03135w_{1,1}^2 - 0.1047w_{1,3}^2 - 0.8886w_{3,1}^2 - 0.1544w_{2,2}^2 - 6.821w_{3,3}^2$$
$$+ 0.1097w_{1,1}w_{1,3} + 0.1207w_{1,1}w_{3,1} + 0.07695w_{1,3}w_{3,3} - 2.862w_{3,1}w_{3,3}$$
$$- 0.04395w_{1,3}w_{3,1} + 0.2398w_{1,1}w_{3,3})$$

$$B_6 = \frac{E}{10^7}(-0.03761w_{1,1}^2 - 0.8202w_{1,3}^2 - 0.08139w_{3,1}^2 - 0.1632w_{2,2}^2 - 5.068w_{3,3}^2$$
$$+ 0.1363w_{1,1}w_{1,3} + 0.1506w_{1,1}w_{3,1} - 3.005w_{1,3}w_{3,3} - 0.000781w_{3,1}w_{3,3}$$
$$- 0.01981w_{1,3}w_{3,1} + 0.2910w_{1,1}w_{3,3})$$

The struts and flanges are considered to be stiff enough in bending to keep straight the four edges ($x = 0$, $x = a$, $y = 0$, $y = a$) of the plate. Equations for the u and v displacement can be obtained from p. 322 of reference 1.

$$\left.\begin{aligned}
\frac{\partial u}{\partial x} &= \epsilon_x' - \frac{1}{2}\left(\frac{\partial w}{\partial x}\right)^2 \\
\frac{\partial v}{\partial y} &= \epsilon_y' - \frac{1}{2}\left(\frac{\partial w}{\partial y}\right)^2 \\
\frac{\partial u}{\partial y} + \frac{\partial v}{\partial x} &= \gamma_{x,y} - \frac{\partial w}{\partial x}\frac{\partial w}{\partial y}
\end{aligned}\right\} \tag{15}$$

Values of u and v can be obtained by substituting equations (4), (6), (7), (8), and (14) into equations (15) and integrating. This gives for the values of u and v at the edges of the plate for $r = \infty$,

$$(u)_{x=o} = 0, \qquad (u)_{x=a} = 0$$

$$(v)_{y=o} = x\,\frac{2.632T}{E}; \qquad (v)_{y=a} = x\,\frac{2.632T}{E} \tag{16a}$$

and for $r = 0.25$

$$(u)_{x=o} = 0; \qquad (u)_{x=a} = 0$$

$$(v)_{y=o} = x\,\frac{2.632T}{E}; \qquad (v)_{y=a} = x\,\frac{2.632T}{E} - \frac{4}{a}\,(0.3313w_{1,1}^2$$

$$+ 2.346w_{1,3}^2 + 0.9678w_{3,1}^2 + 1.325w_{2,2}^2 + 2.982w_{3,3}^2) \tag{16b}$$

It is seen from equations (16) that the edges of the plate corresponding to $x = 0$, $x = a$, $y = 0$, and $y = a$, satisfy the condition of remaining straight after buckling has started.

EQUILIBRIUM OF LATERAL FORCES

After the web plate buckles, the median fiber forces have components which tend to displace elements of the plate laterally from the original plane of the plate. These forces will displace the plate laterally until the bending stiffness of the plate prevents further displacement. This condition is expressed by equation (2).

The lateral deflection (equation(6)) must now be determined in such a way that equation (2) is satisfied. The fact that the series expression for w (equation (6)) has been limited to only the first five terms, makes it impossible to identically satisfy equation (2). Except for a small unequilibrated lateral pressure p of order higher than 3, however, it can be shown by expanding F into trigonometric series and by substituting equations (6), (7), (8), and (14) into equation (2), as is done in reference 8, that equation (2) is satisfied.

for $r = \infty (w_{1,3} = w_{3,1})$, when

$$
\left.
\begin{aligned}
0 &= 1.973w_{1,1}^3 + w_{1,1}^2(-1.657w_{1,3} - 0.1360w_{3,3}) + w_{1,1}(1.4815h^2 \\
&\quad + 25.69w_{1,3}^2 + 15.16w_{3,3}^2 + 8.09w_{2,2}^2 - 8.88w_{1,3}w_{3,3}) \\
&\quad - 0.5840w_{2,2}\frac{\tau a^2}{E} - 13.147w_{1,3}^3 - 0.00853w_{3,3}^3 + 24.36w_{1,3}^2w_{3,3} \\
&\quad + 1.681w_{3,3}^2w_{1,3} + 8.80w_{2,2}^2w_{1,3} + 3.602w_{2,2}^2w_{3,3} \\
0 &= 123.3w_{1,3}^3 + w_{1,3}^2(-19.72w_{1,1} - 61.28w_{3,3}) + w_{1,3}(37.04h^2 \\
&\quad + 12.85w_{1,1}^2 + 156.6w_{3,3}^2 + 74.64w_{2,2}^2 + 24.36w_{1,1}w_{3,3}) \\
&\quad + 1.051w_{2,2}\frac{\tau a^2}{E} - 0.2761w_{1,1}^3 + 0.0235w_{3,3}^3 - 2.220w_{1,1}^2w_{3,3} \\
&\quad + 0.8387w_{3,3}^2w_{1,1} + 4.402w_{2,2}^2w_{1,1} + 15.62w_{2,2}^2w_{3,3} \\
0 &= 159.3w_{3,3}^3 + w_{3,3}^2(-0.02561w_{1,1} + 0.1410w_{1,3}) + w_{3,3}(120h^2 \\
&\quad + 313.2w_{1,3}^2 + 81.90w_{2,2}^2 + 3.358w_{1,1}w_{1,3} + 15.16w_{1,1}^2) \\
&\quad - 1.892w_{2,2}\frac{\tau a^2}{E} - 0.0453w_{1,1}^3 - 40.85w_{1,3}^3 - 4.439w_{1,1}^2w_{1,3} \\
&\quad + 24.36w_{1,3}^2w_{1,1} + 5.599w_{2,2}^2w_{1,1} + 31.22w_{2,2}^2w_{1,3} \\
0 &= 31.47w_{2,2}^3 + w_{2,2}(23.704h^2 + 8.090w_{1,1}^2 + 149.3w_{1,3}^2 \\
&\quad + 81.90w_{3,3}^2 + 17.61w_{1,1}w_{1,3} + 7.201w_{1,1}w_{3,3} + 62.45w_{1,3}w_{3,3}) \\
&\quad + \frac{\tau a^2}{E}(-0.5840w_{1,1} + 2.102w_{1,3} - 1.892w_{3,3})
\end{aligned}
\right\} \quad (17a)
$$

and for $r = 1/4$, when

$$
\left.
\begin{aligned}
0 = {} & 1.184w_{1,1}^3 - w_{1,1}^2(0.8046w_{1,3} + 0.8132w_{3,1} + 0.1021w_{3,3}) + w_{1,1}(6.147w_{1,3}^2 \\
& + 9.424w_{3,1}^2 + 4.946w_{2,2}^2 + 7.997w_{3,3}^2 - 4.438w_{3,1}w_{3,3} - 4.5604w_{1,3}w_{3,3} \\
& + 2.129w_{1,3}w_{3,1} + 1.4815h^2) - 0.08137w_{1,3}^3 - 0.05188w_{3,1}^3 - 0.00543w_{3,3}^3 \\
& - 6.524w_{1,3}^2w_{3,1} + 0.1422w_{1,3}^2w_{3,3} - 6.448w_{1,3}w_{3,1}^2 + 4.402w_{1,3}w_{2,2}^2 + 0.7930w_{1,3}w_{3,3}^2 \\
& + 0.09027w_{3,1}^2w_{3,3} + 4.404w_{3,1}w_{2,2}^2 + 0.4790w_{3,1}w_{3,3}^2 + 23.69w_{1,3}w_{3,1}w_{3,3} \\
& + 3.605w_{2,2}^2w_{3,3} - 0.5840w_{2,2}\frac{\tau a^2}{E} \\
0 = {} & 18.894w_{2,2}^3 + w_{2,2}(4.945w_{1,1}^2 + 36.325w_{1,3}^2 + 49.387w_{3,1}^2 + 53.584w_{3,3}^2 \\
& + 8.803w_{1,1}w_{1,3} + 8.808w_{3,1}w_{1,1} + 7.207w_{1,1}w_{3,3} + 31.23w_{1,3}w_{3,3} + 31.19w_{3,1}w_{3,3} \\
& + 32.16w_{1,3}w_{3,1} + 23.704h^2) + \frac{\tau a^2}{E}(-0.5840w_{1,1} + 1.051w_{1,3} + 1.051w_{3,1} - 1.892w_{3,3}) \\
0 = {} & 95.56w_{3,3}^3 + w_{3,3}^2(-0.01629w_{1,1} + 0.05922w_{1,3} + 0.08791w_{3,1}) + w_{3,3}(7.995w_{1,1}^2 \\
& + 106.16w_{1,3}^2 + 134.05w_{3,1}^2 + 53.585w_{2,2}^2 + 1.586w_{1,1}w_{1,3} + 0.9578w_{1,1}w_{3,1} \\
& + 0.4191w_{1,3}w_{3,1} + 120.0h^2) - 21.03w_{1,3}^3 - 20.70w_{3,1}^3 - 0.03405w_{1,1}^3 - 2.280w_{1,1}^2w_{1,3} \\
& - 2.219w_{1,1}^2w_{3,1} + 0.1426w_{1,1}w_{1,3}^2 + 0.09046w_{1,1}w_{3,1}^2 + 3.602w_{1,1}w_{2,2}^2 + 0.6284w_{1,3}^2w_{3,1} \\
& + 0.3717w_{1,3}w_{3,1}^2 + 15.613w_{1,3}w_{2,2}^2 + 15.59w_{3,1}w_{2,2}^2 + 23.69w_{1,1}w_{1,3}w_{3,1} - 1.892w_{2,2}\frac{\tau a^2}{E} \\
0 = {} & 30.235w_{1,3}^3 + w_{1,3}^2(-0.2443w_{1,1} - 0.3904w_{3,1} - 63.09w_{3,3}) + w_{1,3}(6.147w_{1,1}^2 \\
& + 37.897w_{3,1}^2 + 106.156w_{3,3}^2 + 36.34w_{2,2}^2 - 13.05w_{1,1}w_{3,1} + 0.2849w_{1,1}w_{3,3} \\
& + 1.258w_{3,1}w_{3,3} + 37.04h^2) - 0.2682w_{1,1}^3 - 0.07916w_{3,1}^3 + .01976w_{3,3}^3 + 1.064w_{1,1}^2w_{3,1} \\
& - 2.280w_{1,1}^2w_{3,3} + 4.401w_{1,1}w_{2,2}^2 - 6.448w_{1,1}w_{3,1}^2 + 0.7927w_{1,1}w_{3,3}^2 + 0.3724w_{3,1}^2w_{3,3} \\
& + 16.08w_{3,1}w_{2,2}^2 + 0.2096w_{3,1}w_{3,3}^2 + 15.62w_{2,2}^2w_{3,3} + 23.69w_{1,1}w_{3,1}w_{3,3} + 1.051w_{2,2}\frac{\tau a^2}{E} \\
0 = {} & 62.735w_{3,1}^3 + w_{3,1}^2(-0.1558w_{1,1} - 0.2367w_{1,3} - 62.09w_{3,3}) + w_{3,1}(3.423w_{1,1}^2 + 37.898w_{1,3}^2 \\
& + 49.405w_{2,2}^2 + 134.05w_{3,3}^2 - 12.30w_{1,1}w_{1,3} + 0.1808w_{1,1}w_{3,3} + 0.7443w_{1,3}w_{3,3} + 37.04h^2) \\
& - 0.2711w_{1,1}^3 - 0.1303w_{1,3}^3 + 0.02933w_{3,3}^3 + 1.064w_{1,1}^2w_{1,3} - 2.219w_{1,1}^2w_{3,3} - 6.524w_{1,1}w_{1,3}^2 \\
& + 4.403w_{1,1}w_{2,2}^2 + 0.4787w_{1,1}w_{3,3}^2 + 0.6293w_{1,3}^2w_{3,3} + 16.08w_{1,3}w_{2,2}^2 + 0.2095w_{1,3}w_{3,3}^2 \\
& + 15.59w_{2,2}^2w_{3,3} + 23.69w_{1,1}w_{1,3}w_{3,3} + 1.051w_{2,2}\frac{\tau a^2}{E}
\end{aligned}
\right\} \quad (17b)
$$

BENDING MOMENT AND SHEARING FORCE IN FLANGE

A flange of the beam (fig. 1) can itself be considered as a beam supported at the strut points and subjected to a lateral load by the median fiber tension in the shear web. Before buckling, the web carries all the shearing force in shear and therefore there is no tendency to bend the flange. After buckling, however, the web carries some of the shearing force by developing a diagonal tension field. This diagonal tension field tends to draw the two flanges together.

The flange bending moment will be considered as positive when it curves the lower flange concave upward or the upper flange concave downward. The shearing force in either flange will be considered positive if it tends to support an external load Q, directed as shown in figure 1.

If use is made of the fact that the flange bending moment is the same at each strut point, the shearing forces in the upper and lower flanges are, respectively,

$$\left.\begin{aligned} &\int_x^a h(\sigma_y')_{y=a}\,dx - \frac{1}{a}\int_0^a h(\sigma_y')_{y=a}\,x\,dx \\ &\text{and} \\ &\frac{1}{a}\int_0^a h(\sigma_y')_{y=0}\,x\,dx - \int_x^a h(\sigma_y')_{y=0}\,dx \end{aligned}\right\} \tag{18}$$

The bending moment in the flange is determined by making the slope of the flange the same at each strut point. This gives for the bending moments in the upper and lower flanges, respectively,

$$\left.\begin{aligned} M_{y=a} &= \frac{1}{2}\int_0^a h(\sigma_y')_{y=a}\,x\left(1-\frac{x}{a}\right)dx + \frac{x}{a}\int_0^a h(\sigma_y')_{y=a}\,x\,dx \\ &\qquad - \int_0^x dx \int_x^a h(\sigma_y')_{y=a}\,dx, \\ M_{y=o} &= \frac{1}{2}\int_0^a h(\sigma_y')_{y=o}\,x\left(1-\frac{x}{a}\right)dx + \frac{x}{a}\int_0^a h(\sigma_y')_{y=o}\,x\,dx \\ &\qquad - \int_0^x dx \int_x^a h(\sigma_y')_{y=o}\,dx \end{aligned}\right\} \tag{19}$$

Substituting for $(\sigma_y^1)_{y=o}$ from equations (3) and (7) and performing the integrations in equation (19) gives for $M_{y=o}$

$$
\begin{aligned}
M_{y=o} &= a^2 h\bar{\sigma}_y \left(\frac{1}{12} - \frac{x}{2a} + \frac{x^2}{2a^2}\right) + h\left(\frac{2x}{a} - 1\right) \sum_{m=1,3}^{5} \sum_{n=0}^{6} b_{m,n} \\
&+ h \sum_{m=1}^{6} \sum_{n=0}^{6} b_{m,n} \cos \frac{m\pi x}{a} \\
&+ h \sum_{m=1,3}^{5} A_m \left[\left(\frac{1-\mu}{1+\mu} - \frac{m\pi}{2}\tanh\frac{m\pi}{2}\right) \sinh\frac{m\pi}{2} + \frac{m\pi}{2}\cosh\frac{m\pi}{2}\right]\left(1 - \frac{2x}{a} - \cos\frac{m\pi x}{a}\right) \\
&+ h \sum_{m=2,4}^{6} A_m \left[\left(\frac{1-\mu}{1+\mu} - \frac{m\pi}{2}\coth\frac{m\pi}{2}\right) \cosh \frac{m\pi}{2} + \frac{m\pi}{2} \sinh \frac{m\pi}{2}\right] \cos \frac{m\pi x}{a} \\
&+ h \sum_{n=1,3}^{5} B_n \left\{\left[\frac{1-\mu}{1+\mu} - \frac{n\pi}{2}\tanh\frac{n\pi}{2}\right] \left[\left(1 - \frac{2x}{a}\right) \sinh\frac{n\pi}{2} + \sinh n\pi\left(\frac{x}{a} - \frac{1}{2}\right)\right]\right. \\
&\left. + n\pi \left(\frac{x}{a} - \frac{1}{2}\right) \left[\cosh n\pi \left(\frac{x}{a} - \frac{1}{2}\right) - \cosh \frac{n\pi}{2}\right]\right\} \\
&+ h \sum_{n=2,4}^{6} B_n \left\{\left[\frac{1-\mu}{1+\mu} - \frac{n\pi}{2} \coth \frac{n\pi}{2}\right] \cosh n\pi \left(\frac{x}{a} - \frac{1}{2}\right) + \frac{4\mu}{n\pi(1+\mu)} \sinh\frac{n\pi}{2}\right. \\
&\left. + n\pi \left(\frac{x}{a} - \frac{1}{2}\right) \sinh n\pi \left(\frac{x}{a} - \frac{1}{2}\right)\right\} \qquad (19a)
\end{aligned}
$$

SHEAR LOAD CARRIED BY BEAM

The beam (fig. 1) supports a shear load Q. At any vertical section through the beam this load is partially carried by shear in the web and partially by shear in the flanges. Part of the shear in the web may be considered due to the diagonal tension after buckling.

The shear load carried by the flanges is obtained by adding equations (18). The shear load carried by the web is

$$-\int_0^a h\ \tau'_{xy}\ dy \tag{20}$$

Adding equations (18) and (20), substituting for σ'_y and τ'_{xy} their values as given by equations (3), (7), (8), (14a), and (14b), and integrating gives

for $r = \infty\ (w_{1,3} = w_{3,1})$

$$Q = -\tau ah + w_{2,2}\frac{Eh}{a}\left(1.350w_{1,1} - 4.862w_{1,3} + 4.376w_{3,3}\right) \tag{21a}$$

and for $r = 1/4$

$$Q = -\tau ah + w_{2,2}\frac{Eh}{a}\left(1.349w_{1,1} - 2.432w_{1,3} - 2.430w_{3,1} + 4.372w_{3,3}\right) \tag{21b}$$

SHEARING DEFORMATION OF BEAM

The shearing forces acting on the end of the beam cause it to shear downward as shown in figure 1. The amount of the downward displacement is $(v)_{y=0}$ in equations (16a) and (16b). This gives

$$(v)_{y=0} = 2.632\frac{\tau x}{E} = \bar{\gamma}x; \qquad \bar{\gamma} = 2.632\frac{\tau}{E} \tag{22}$$

where $\bar{\gamma}$ is the shear deformation of the beam.

EFFECTIVE WIDTH IN SHEAR

The loss in shear stiffness of the beam after buckling of the web may be considered as a loss in effective width of the sheet. The effective width ratio in shear for a given

shearing deformation $\bar{\gamma}$ will be defined as the ratio of the load actually carried by the beam to the load which might have been carried had the web not buckled.

The load actually carried by the beam is given by equations (21a) and (21b). The shearing deformation of the beam is $\bar{\gamma}$ (equation 22). From equations (3), (4), and (7), therefore, a load τah might have been carried with a shear deformation $\bar{\gamma}$ if the web had not buckled. The effective width ratio is, therefore,

$$\text{Effective width ratio} = Q/\tau ah \tag{23}$$

Substituting for Q from equations (21a) and (21b) gives for $r = \infty\ (w_{1,3} = w_{3,1})$

Effective width ratio

$$= 1 - \frac{E}{\tau a^2} w_{2,2}(1.350w_{1,1} - 4.862w_{1,3} + 4.376w_{3,3}) \tag{24a}$$

and for $r = 1/4$

Effective width ratio

$$= 1 - \frac{E}{\tau a^2} w_{2,2}(1.349w_{1,1} - 2.432w_{1,3} - 2.430w_{3,1} + 4.372w_{3,3}) \tag{24b}$$

COMPRESSIVE FORCE IN VERTICAL STRUT

After buckling of the web, the diagonal tension field tends to draw the two flanges of the beam together. This action is counteracted by the vertical struts which hold the flanges apart. The magnitude of the resulting compressive force in the strut is given by equation (12). Substituting for $\bar{\sigma}_y$, B_2, B_4, and B_6 the values given in equations (14a) and (14b) gives

for $r = \infty (w_{1,3} = w_{3,1})$

$$P = \frac{Eh}{a}\Big\{(1.804w_{1,1}^2+18.04w_{1,3}^2+16.24w_{3,3}^2+7.217w_{2,2}^2)$$

$$+ \cos\frac{2\pi y}{a}(-0.0846w_{1,1}^2-0.2858w_{1,3}^2-0.0171w_{3,3}^2-0.0189w_{2,2}^2$$

$$+ 0.815w_{1,1}w_{1,3}+0.708w_{1,1}w_{3,3}+3.100w_{1,3}w_{3,3})$$

$$+ \cos\frac{4\pi y}{a}(-0.0047w_{1,1}^2-0.2467w_{1,3}^2-0.0170w_{3,3}^2-0.1538w_{2,2}^2$$

$$-0.0284w_{1,1}w_{1,3}+0.0165w_{1,1}w_{3,3}-0.623w_{1,3}w_{3,3})$$

$$+\cos\frac{6\pi y}{a}(-0.0019w_{1,1}^2-0.0419w_{1,3}^2-0.2235w_{3,3}^2-0.0075w_{2,2}^2$$

$$+ 0.0148w_{1,1}w_{1,3} + 0.0148w_{1,1}w_{3,3}- 0.0814w_{1,3}w_{3,3})\Big\} \quad (25a)$$

and for $x = 1/4$

$$
\begin{aligned}
P = \frac{Eh}{a}\Big\{ & (0.3313w_{1,1}^2+2.346w_{1,3}^2+0.9678w_{3,1}^2+1.325w_{2,2}^2+2.982w_{3,3}^2) \\
& + \cos\frac{2\pi y}{a}(-0.04840w_{1,1}^2-0.05979w_{1,3}^2-0.3767w_{3,1}^2-0.01014w_{2,2}^2 \\
& \qquad -0.00919w_{3,3}^2+0.2862w_{1,1}w_{1,3}+0.1798w_{1,1}w_{3,1} \\
& \qquad +0.2051w_{1,3}w_{3,3}+1.566w_{3,1}w_{3,3}+0.3741w_{1,3}w_{3,1} \\
& \qquad +0.4043w_{1,1}w_{3,3}) \\
& + \cos\frac{4\pi y}{a}(-0.003098w_{1,1}^2-0.02441w_{1,3}^2-0.004807w_{3,1}^2 \\
& \qquad -0.1124w_{2,2}^2-0.01203w_{3,3}^2-0.03866w_{1,1}w_{1,3} \\
& \qquad +0.01444w_{1,1}w_{3,1}+0.05847w_{1,3}w_{3,3}-0.5269w_{3,1}w_{3,3} \\
& \qquad -0.1501w_{1,3}w_{3,1}+0.009109w_{1,1}w_{3,3}) \\
& + \cos\frac{6\pi y}{a}(-0.001334w_{1,1}^2-0.02910w_{1,3}^2-0.002888w_{3,1}^2-0.005790w_{2,2}^2 \\
& \qquad -0.1798w_{3,3}^2+0.004836w_{1,1}w_{1,3}+0.005350w_{1,1}w_{3,1} \\
& \qquad -0.07114w_{1,3}w_{3,3}-0.00002696w_{3,1}w_{3,3} \\
& \qquad -0.0007029w_{1,3}w_{3,1}+0.01032w_{1,1}w_{3,3})\Big\}
\end{aligned}
\tag{25b}
$$

Stress at Center of Shear Bay

Examination of beams which have severe shear buckles indicates that the maximum membrane stresses are likely to

occur at the center of the shear bay with the line of failure running at nearly 45° to the flanges.

The stress at the center of the plate is obtained from equations (3), (7), (8), and (14) by letting $x = y = a/2$. This gives

for $r = \infty (w_{1,3} = w_{3,1})$

$$\left.\begin{aligned}
(\sigma'_x = \sigma'_y)_{\substack{x=a/2\\y=a/2}} &= \frac{E}{a^2}(3.069w_{1,1}^2 + 50.22w_{1,3}^2 + 27.35w_{3,3}^2 + 2.278w_{2,2}^2 \\
&\quad -15.59w_{1,1}w_{1,3} + 4.187w_{1,1}w_{3,3} - 56.24w_{1,3}w_{3,3}) \\
(\tau'_{xy})_{\substack{x=a/2\\y=a/2}} &= \tau + \frac{E}{a^2}w_{2,2}(2.267w_{1,1} + 25.80w_{1,3} - 5.775w_{3,3})
\end{aligned}\right\} \quad (26a)$$

and for $r = 1/4$

$$\left.\begin{aligned}
(\sigma'_x)_{\substack{x=a/2\\y=a/2}} &= \frac{E}{a^2}(2.586w_{1,1}^2 + 14.26w_{1,3}^2 + 11.58w_{3,1}^2 + 0.4213w_{2,2}^2 \\
&\quad +23.15w_{3,3}^2 - 2.673w_{1,1}w_{1,3} - 7.823w_{1,1}w_{3,1} + 4.326w_{1,1}w_{3,3} \\
&\quad +24.59w_{1,3}w_{3,1} - 45.57w_{1,3}w_{3,3} - 9.942w_{3,1}w_{3,3}) \\
(\sigma'_y)_{\substack{x=a/2\\y=a/2}} &= \frac{E}{a^2}(1.597w_{1,1}^2 + 13.75w_{1,3}^2 + 2.186w_{3,1}^2 - 3.612w_{2,2}^2 + 14.09w_{3,3}^2 \\
&\quad -2.663w_{1,1}w_{1,3} - 8.008w_{1,1}w_{3,1} + 4.176w_{1,1}w_{3,3} \\
&\quad +24.48w_{1,3}w_{3,1} - 47.15w_{1,3}w_{3,3} - 9.056w_{3,1}w_{3,3}) \\
(\tau'_{xy})_{\substack{x=a/2\\y=a/2}} &= \tau + \frac{E}{a^2}w_{2,2}(2.268w_{1,1} + 12.90w_{1,3} + 12.90w_{3,1} - 5.776w_{3,3})
\end{aligned}\right\} \quad (26b)$$

The maximum and minimum principal stresses at the center of the plate may be obtained from equations (26a) and (26b) by the equations on page 19 of reference 9,

$$\left.\begin{aligned} \sigma'_{\substack{min\\max}} &= \frac{\sigma'_x + \sigma'_y}{2} \pm \sqrt{\left(\frac{\sigma'_x - \sigma'_y}{2}\right)^2 + (\tau'_{xy})^2} \\ \tan 2\alpha &= 2\,\frac{\tau'_{xy}}{\sigma'_x - \sigma'_y} \end{aligned}\right\} \quad (27)$$

where α is the angle between the x-axis and the direction of a principal stress.

Stress at Corner of Shear Bay

The stress at the corner of the shear bay must be mainly a shearing stress, since the principal deformation is a change in angle between the horizontal flange and the vertical struts. The boundary conditions of zero strain parallel to the flange and of strain parallel to the strut equal to the strain in the strut were only partially satisfied (see equations (9), (13), (14a), and (14b)); so small residual stresses in the x and y directions are left. A measure of the degree to which the boundary equations are satisfied is the smallness of these residuals in the case where $r = \infty$. These are computed later in the paper and appear in the second and third columns of tables 3a and 3b.

The stress at the corner of the plate is obtained from equations (3), (7), (8), (14a), and (14b) by letting $x = 0$, $y = a$. This gives

for $r = \infty$ $(w_{1,3} = w_{3,1})$

$$\left.\begin{aligned} (\sigma'_x = \sigma'_y)_{\substack{x=0\\y=a}} &= \frac{E}{a^2}(0.157w_{1,1}^2 + 1.94w_{1,3}^2 + 2.14w_{3,3}^2 + 0.832w_{2,2}^2 \\ &\quad - 1.11w_{1,1}w_{1,3} - 1.18w_{1,1}w_{3,3} - 0.50w_{1,3}w_{3,3} \\ &\quad + 0.732w_{1,1}w_{2,2} - 0.94w_{1,3}w_{2,2} + 1.96w_{3,3}w_{2,2}) \\ (\tau'_{xy})_{\substack{x=0\\y=a}} &= \bar{\tau} \end{aligned}\right\} \quad (28a)$$

and for $r = 1/4$

$$
\left.
\begin{aligned}
(\sigma_x')_{\substack{x=0\\y=a}} &= \frac{E}{a^2}(-0.2889w_{1,1}^2-12.42w_{1,3}^2+9.593w_{3,1}^2-1.029w_{2,2}^2 \\
&\quad -2.103w_{3,3}^2-0.9318w_{1,1}w_{1,3}-0.3613w_{1,1}w_{3,1} \\
&\quad -1.360w_{1,1}w_{3,3}+0.1806w_{1,3}w_{3,1}+6.160w_{1,3}w_{3,3} \\
&\quad -7.493w_{3,1}w_{3,3}+0.7299w_{2,2}w_{1,1}+7.324w_{1,3}w_{2,2} \\
&\quad -8.273w_{3,1}w_{2,2}+1.945w_{2,2}w_{3,3}) \\
(\sigma_y')_{\substack{x=0\\y=a}} &= \frac{E}{a^2}(-1.116w_{1,1}^2-9.080w_{1,3}^2-2.108w_{3,1}^2-4.572w_{2,2}^2 \\
&\quad -10.35w_{3,3}^2-1.5434w_{1,1}w_{1,3}-1.290w_{1,1}w_{3,1} \\
&\quad -2.799w_{1,1}w_{3,3}-0.1693w_{1,3}w_{3,1}-1.067w_{1,3}w_{3,3} \\
&\quad -4.157w_{3,1}w_{3,3}+0.7298w_{1,1}w_{2,2}-0.6991w_{1,3}w_{2,2} \\
&\quad -0.2494w_{3,1}w_{2,2}+1.945w_{2,2}w_{3,3}) \\
(\tau_{xy}')_{\substack{x=0\\y=a}} &= \bar{\tau}
\end{aligned}
\right\} \quad (28b)
$$

Depth of Buckle

The contour of the buckle in the shear bay is given by equation (6). The depth of the buckle at the center of the bay is obtained by setting $x = a/2$ and $y = a/2$. This gives

$$w_{center} = w_{1,1}-w_{1,3}-w_{3,1}+w_{3,3} \tag{29}$$

NUMERICAL SOLUTION

Deflection Coefficients

The deflection coefficients are obtained by solution of the simultaneous equations (17a), (17b). These equations were solved by a method of successive approximation, using the following steps:

1. Divide each of equations (17a) and (17b) by h^3.

2. Estimate values of $w_{1,1}/h$, $w_{1,3}/h$, $w_{3,1}/h$, $w_{3,3}/h$, $\tau a^2/Eh^2$, corresponding to a given value of $w_{2,2}/h$.

3. Expand the right-hand side of each of equations (17a) and (17b) in a Taylor series in the neighborhood of the estimated values of $w_{1,1}/h$, $w_{1,3}/h$, $w_{3,1}/h$, $w_{3,3}/h$, and $\tau a^2/Eh^2$, omitting the square and higher order terms.

4. Solve the resulting linear equations for the difference between the chosen values of $w_{1,1}/h$, $w_{1,3}/h$, $w_{3,1}/h$, $w_{3,3}/h$, $\tau a^2/Eh^2$ and the improved values. (Crout's method, reference 10, was used for this.)

5. Repeat until the estimated error is less than 0.2 percent. The convergence was rapid; so one or two trials usually were sufficient to give an accurate answer.

The results of the computation were checked by substituting the answers in the original equations (17a) and (17b). The results are given in tables 1a and 1b for values of the shear load Q up to about seven times the critical value for buckling. The value of $\overline{\gamma}$ was computed from τ by using equation (22); Q was computed from τ, $w_{1,1}$, $w_{1,3}$, $w_{3,1}$, $w_{3,3}$, and $w_{2,2}$ by using equations (21a) and (21b).

Median Fiber Stresses at Center of Shear Web

The median-fiber stresses at the center of the shear web were computed from equations (26a) and (26b) and tables 1a and 1b. The maximum and minimum principal stresses then were computed from equation (27). These stresses are given in tables 2a and 2b and are plotted against the shear load Q in

dimensionless form in figure 2. When $r = \infty$, the direction of the maximum principal stress forms an angle of 45° with the flanges for all loads; when $r = 1/4$, however, the angle is 45° at the buckling load and decreases to 39° 8' as the load is increased to five times the buckling load.

As might be expected, the maximum principal stress (corresponding to tension along the wrinkle) continues to rise after buckling while the minimum principal stress (corresponding to compression across the wrinkle) remains nearly constant after buckling.

The reinforcement ratio r has only a small effect on the web stresses at the center of the shear bay. (See fig. 2.) The drop in tensile stress at the center when the reinforcement ratio changes from 1/4 to ∞ is only 7 percent at a shear load of $45\ Eh^3/a$.

Median Fiber Stresses at Corner of Shear Web

The median-fiber stresses at the corner of the shear web were computed from equations (28a) and (28b) and tables 1a and 1b. The maximum and minimum principal stresses then were computed from equation (27). These stresses are given in tables 3a and 3b and are plotted against the shear load Q in dimensionless form in figure 3. The direction of the maximum principal stress forms an angle of 45° with the flanges for all loads when $r = \infty$; when $r = 1/4$, however, the angle is 45° up to the buckling load and decreases to 41° 4' as the load is increased to five times the buckling load.

Comparison of figures 2 and 3 shows that the maximum tensile stress occurs at the center of the plate while the maximum compressive stress occurs in the corner.

The reinforcement ratio r has an appreciable effect on the stress in the corner. (See fig. 3.) The increase in compressive stress at the corner when the reinforcement ratio r changes from ∞ to 1/4 is 40 percent at a load $Q = 45\ Eh^3/a$.

Effective Width of the Sheet

The effective width of the sheet (corresponding to the width of unbuckled sheet which would give the same shear deformation as the actual buckled sheet) was computed from

equations (24a) and (24b) and tables 1a and 1b. The ratio of the effective width to the actual width is given in tables 3a and 3b and is plotted in figure 4 against the shear deformation ratio $\bar{\gamma}\frac{a^2}{h^2}$. Changing the strut area so that the reinforcement ratio $r = 1/4$ instead of ∞ causes a drop in effective width ratio from 0.88 to 0.81 for a shear deformation $\bar{\gamma} = 140\ h^2/a^2$.

Figure 4 shows that the effective width decreases slowly with increase in the shear deformation. In this connection it should be remembered that the present paper is limited to edge reinforcements which are rigid against bending in the plane of the web. It should not be assumed that the effective width will be as high as in figure 4 when the reinforcements allow bending in the plane of the web.

Bending Moment in Flange

The bending moments in the lower flange, due to the web stresses σ_y' acting normal to the flange, are given by equation (19a). This equation does not take account of the fact that the web shear stress τ_{xy}' contributes to the bending moment when the neutral axis of the flange does not coincide with the edge of the shear web. The bending moments along the flange $y = 0$ computed from equation (19a) using equations (8), (14a), (14b), and tables 1a and 1b, are given in figure 5 for $r = 1/4$, $Q = 45.37Eh^3/a$ and for $r = \infty$, $Q = 47.22Eh^3/a$. The maximum moment occurs at the struts, $x = 0$, $x = a$. The distribution of moment is similar to that in a beam with clamped ends under a uniformly distributed load. Although the shear load Q is nearly the same in the two cases, the moments for $r = \infty$ are nearly twice the moments for $r = 1/4$; the decrease in cross-sectional area of the struts causes a marked decrease in flange bending moment.

Compressive Force in Strut

The compressive force in the strut is given by equation (12). The distribution of compressive force P along the strut was computed from equation (12) using equations (14a) and (14b) and tables 1a and 1b. The results are plotted in figure 6 for $r = 1/4$, $Q = 45.37Eh^3/a$ and for $r = \infty$, $Q = 47.22Eh^3/a$. The variation in compressive force P along

the strut is 19 percent when $r = 1/4$ and only 8 percent when $r = \infty$. The maximum force occurs at the center of the strut, $y = a/2$.

The maximum force $P_{y=a/2}$ was computed for various loads. It is plotted against load in figure 7. For a given load Q on the beam, the force $P_{y=a/2}$ in the strut is about three times as great when $r = \infty$ as when $r = 1/4$. When $r = 1/4$ a considerable portion of the force holding the flanges apart seems to be carried by the sheet adjacent to the strut.

Shear Deformation of Beam

The shear deformation $\bar{\gamma}$ of the beam and the shear load Q are given in dimensionless form in tables 1a and 1b. They are plotted against each other in figure 8 for $r = 1/4$ and $r = \infty$. The deformation when $r = 1/4$ is only about 9 percent greater than when $r = \infty$. The cross-sectional area of the strut apparently has only a minor effect on the stiffness of beams with buckled webs resisting shear when the strut spacing equals the beam depth and when the flanges are very stiff.

After buckling, the effective shear stiffness of the web is decreased about 8 percent for $r = \infty$ and about 12 percent for $r = 1/4$.

Comparison with "Tension Field" Theory

The most widely used concept in predicting the behavior of a shear web after buckling is that of the "tension field" originated by Wagner. Wagner (reference 2) postulated that the shear load carried by a thin sheet web after buckling is chiefly carried by tension in the direction of the sheet buckles. Improvements of Wagner's original theory to take account more adequately of the case of an incompletely developed tension field have been derived in references 11, 12, and 13.

Kuhn (references 11 and 12) has developed a semiempirical treatment for the action of shear webs in incomplete diagonal tension. Kuhn's results are plotted as curves C in figures 9, 10, and 11 for comparison with the present work. The agreement is excellent in the practical case where $r = 1/4$ except

for the stress in the corner of the buckle (curve B). In the extreme case where $r = \infty$, however, the agreement is not so good.

Langhaar (reference 13) takes account of reinforcements and assumes that a compressive stress equal to the critical shear stress acts perpendicular to the buckles. He neglects the effect of Poisson's ratio ($\mu = 0$). Langhaar's results are plotted as curves D in figures 9, 10, and 11 for comparison with the present work. The agreement is excellent for the stress at the center of the panel (curve A, fig. 9). It is not quite so good for the shear deformation (fig. 11). For the force in the strut (fig. 10), Langhaar's results are nearly twice as high as those of the present paper.

The preceding comparisons of Wagner's theory, as developed by Kuhn and by Langhaar, with the more complete analysis given in the present paper for the special case of a square plate, indicates that Wagner's theory as developed by Kuhn is in best agreement with the present paper in the practical case $r = 1/4$. Kuhn's theory is in especially good agreement for the force in the strut when $r = 1/4$.

National Bureau of Standards,
Washington, D. C., July 1, 1944.

REFERENCES

1. Timoshenko, S.: Theory of Elastic Stability. McGraw-Hill Book Co., Inc., 1936.

2. Wagner, Herbert: Flat Sheet Metal Girders with Very Thin Metal Web.
   Part I – General Theories and Assumptions. NACA TM No. 604, 1931.
   Part II – Sheet Metal Girders with Spars Resistant to Bending – Oblique Uprights – Stiffness. NACA TM No. 605, 1935.
   Part III – Sheet Metal Girders with Spars Resistant to Bending – The Stress in Uprights – Diagonal Tension Fields. NACA TM No. 606, 1931.

3. Kuhn, Paul: A Summary of Design Formulas for Beams Having Thin Webs in Diagonal Tension. NACA TN No. 469, 1933.

4. Schapitz, E.: The Twisting of Thin-Walled Stiffened Circular Cylinders. NACA TM No. 878, 1938.

5. Moore, R. L.: An Investigation of the Effectiveness of Stiffeners of Shear-Resistant Plate-Girder Webs. NACA TN No. 862, 1942.

6. Lahde, R. and Wagner, H.: Tests for the Determination of the Stress Condition in Tension Fields. NACA TM No. 809, 1936.

7. Seydel, E.: Uber das Ausbeulen von rechteckigen isotropen oder orthogonal-anistropen Platten bei Schubbeanspruchung. Ing.-Archiv, vol. 4, 1933, pp. 169-191.

8. Levy, Samuel: Bending of Rectangular Plates with Large Deflections. NACA Rep. No. 737, 1942. (Issued also as NACA TN No. 846, 1942.)

9. Timoshenko, S.: Theory of Elasticity. McGraw-Hill Book Co. Inc., 1934.

10. Crout, Prescott D.: A Short Method for Evaluating Determinants and Solving Systems of Linear Equations with Real or Complex Coefficients. Trans. A.I.E.E., vol. 60, 1941.

11. Kuhn, Paul: Investigations of the Incompletely Developed Plane Diagonal-Tension Field. NACA Rep. No. 697, 1940.

12. Kuhn, Paul, and Chiarito, Patrick T.: The Strength of Plane Web Systems in Incomplete Diagonal Tension. NACA ARR, Aug. 1942.

13. Langhaar, H. L.: Theoretical and Experimental Investigations of Thin-Webbed Plate-Girder Beams. Trans. A.S.M.E., vol. 65, 1943, pp. 799-802.

Table 1a - Values of the deflection coefficients as a function of the apparent shearing deformation $\bar{\gamma}$ or of the shear load Q for r = ∞.

$\frac{Qa}{Eh^3}$	$-\frac{\bar{\gamma}a^2}{h^2}$	$\frac{w_{1,1}}{h}$	$\frac{w_{1,3}}{h}$	$\frac{w_{3,1}}{h}$	$\frac{w_{3,3}}{h}$	$\frac{w_{2,2}}{h}$	$\frac{\bar{\tau}a^2}{Eh^2}$
0	0	0	0	0	0	0	0
8.61	22.68	0	0	0	0	0	-8.61
8.82	23.24	+0.1587	-0.0118	-0.0118	+0.0066	-0.0479	-8.83
9.30	24.61	+ .2922	- .0235	- .0235	+ .0134	- .0931	-9.35
10.01	26.65	.4070	- .0360	- .0360	+ .0210	- .1390	-10.12
10.56	28.25	+ .4764	- .0455	- .0455	+ .0270	- .1722	-10.73
11.01	29.6	.525	- .053	- .053	.032	- .198	-11.23
12.00	32.5	.613	- .069	- .069	.043	- .251	-12.34
13.20	36.0	.694	- .085	- .085	.055	- .303	-13.68
14.02	38.5	.746	- .097	- .097	.065	- .344	-14.63
15.25	42.6	.814	- .115	- .115	.080	- .405	-16.16
16.55	46.2	.881	- .129	- .129	.093	- .453	-17.56
17.86	50.2	.917	- .145	- .145	.107	- .499	-19.06
20.67	58.8	1.006	- .172	- .172	.136	- .593	-22.32
24.30	70.0	1.110	- .206	- .206	.173	- .704	-26.59
28.04	81.6	1.200	- .234	- .234	.209	- .804	-30.99
32.04	94.0	1.284	- .263	- .263	.245	- .900	-35.72
36.60	108.2	1.371	- .291	- .291	.282	- .999	-41.10
41.76	124.3	1.462	- .320	- .320	.322	-1.101	-47.20
47.22	141.3	1.551	- .348	- .348	.361	-1.199	-53.65
53.22	159.9	1.642	- .376	- .376	.401	-1.299	-60.75
59.82	180.4	1.735	- .403	- .403	.442	-1.400	-68.55
66.69	202.0	1.828	- .432	- .432	.482	-1.499	-76.70

Table 1b - Values of the deflection coefficients as a function of the apparent shearing deformation $\bar{\gamma}$ or of the shear load Q for r = 1/4.

$\frac{Qa}{Eh^3}$	$-\frac{\bar{\gamma}a^2}{h^2}$	$\frac{w_{1,1}}{h}$	$\frac{w_{1,3}}{h}$	$\frac{w_{3,1}}{h}$	$\frac{w_{3,3}}{h}$	$\frac{w_{2,2}}{h}$	$\frac{\bar{\tau}a^2}{Eh^2}$
0	0	0	0	0	0	0	0
8.61	22.66	0	0	0	0	0	- 8.61
8.73	23.02	+ .1601	-.01178	-.01174	+.00657	- .0479	- 8.74
9.10	24.12	+ .3196	-.02504	-.02472	+.01411	- .1000	- 9.16
9.61	25.66	+ .4522	-.03844	-.03745	+.02198	- .1500	- 9.75
10.21	27.47	+ .5662	-.0525	-.05035	+.03051	- .2000	-10.44
10.86	29.50	+ .6647	-.06709	-.06326	+.03972	- .2500	-11.20
11.55	31.68	+ .750	-.082	-.076	+.049	- .300	-12.03
12.27	33.98	+ .828	-.097	-.088	+.060	- .350	-12.91
13.02	36.44	+ .898	-.113	-.101	+.071	- .400	-13.84
13.81	39.02	+ .962	-.128	-.113	+.083	- .450	-14.82
14.64	41.75	+1.02	-.144	-.125	+.095	- .500	-15.86
16.40	47.67	+1.129	-.175	-.151	+.122	- .600	-18.11
18.33	54.22	+1.232	-.208	-.169	+.151	- .700	-20.60
20.45	61.47	+1.327	-.240	-.189	+.182	- .800	-23.35
22.77	69.47	+1.419	-.272	-.209	+.214	- .900	-26.39
25.31	78.25	+1.509	-.303	-.2298	+.249	-1.000	-29.73
31.03	98.16	+1.687	-.365	-.267	+.320	-1.200	-37.29
34.25	109.40	+1.775	-.396	-.286	+.358	-1.300	-41.56
41.42	134.43	+1.954	-.458	-.324	+.434	-1.500	-51.07
45.36	148.24	+2.045	-.488	-.343	+.472	-1.600	-56.32

Table 2a - Median-Fiber Stress at Center, $r = \infty$
Maximum and Minimum Principal Stresses
Direction of Principal Stresses

$\frac{Qa}{Eh^3}$	$\frac{\sigma'_x a^2}{Eh^2}$	$\frac{\sigma'_y a^2}{Eh^2}$	$\frac{\tau'_{xy} a^2}{Eh^2}$	$\frac{\sigma'_{min} a^2}{Eh^2}$	$\frac{\sigma'_{max} a^2}{Eh^2}$	α
8.61	0	0	- 8.61	- 8.61	8.61	45°
8.82	.1287	.1287	- 8.83	- 8.70	8.96	"
9.30	.4555	.4555	- 9.35	- 8.89	9.81	"
10.01	.9363	.9363	-10.10	- 9.16	11.04	"
10.56	1.349	1.349	-10.68	- 9.33	12.03	"
11.01	1.701	1.701	-11.16	- 9.46	12.86	"
12.00	2.523	2.523	-12.18	- 9.66	14.70	"
13.20	3.476	3.476	-13.40	- 9.92	16.88	"
14.02	4.253	4.253	-14.22	- 9.97	18.47	"
15.25	5.496	5.496	-15.52	-10.02	21.02	"
16.55	6.712	6.712	-16.71	-10.00	23.42	"
17.86	7.874	7.874	-17.92	-10.05	25.79	"
20.67	10.486	10.486	-20.58	-10.09	31.07	"
24.30	14.233	14.233	-23.92	- 9.69	38.15	"
28.04	18.015	18.015	-27.35	- 9.33	45.37	"
32.04	22.227	22.227	-30.96	- 8.73	53.19	"
36.60	26.924	26.924	-35.08	- 8.16	62.00	"
41.76	32.361	32.361	-39.72	- 7.36	72.08	"
47.22	38.128	38.128	-44.60	- 6.47	82.73	"
53.22	44.479	44.479	-49.98	- 5.50	94.46	"
59.82	51.332	51.332	-55.93	- 4.60	107.26	"
66.69	58.811	58.811	-62.03	- 3.22	120.84	"

Table 2b - Median-Fiber Stress at Center, $r = 1/4$
Maximum and Minimum Principal Stresses
Direction of Principal Stresses

$\frac{Qa}{Eh^3}$	$\frac{\sigma'_x a^2}{Eh^2}$	$\frac{\sigma'_y a^2}{Eh^2}$	$\frac{\tau'_{xy} a^2}{Eh^2}$	$\frac{\sigma'_{min} a^2}{Eh^2}$	$\frac{\sigma'_{max} a^2}{Eh^2}$	α
8.61	0	0	- 8.61	- 8.61	+ 8.61	45°
8.73	+ .10	+ .06	- 8.75	- 8.66	+ 8.83	44° 56'
9.10	+ .42	+ .27	- 9.16	- 8.81	+ 9.51	44° 46'
9.61	+ .89	+ .58	- 9.73	- 9.03	+10.50	44° 32.5'
10.21	+1.46	+ .95	-10.39	- 9.18	+11.61	44° 18'
10.86	+2.12	+1.39	-11.10	- 9.35	+12.87	44° 3'
11.55	+2.86	+1.87	-11.85	- 9.49	+14.23	43° 48'
12.27	+3.67	+2.39	-12.60	- 9.58	+15.66	43° 33'
13.02	+4.55	+2.96	-13.39	- 9.65	+17.17	43° 19'
13.81	+5.49	+3.58	-14.19	- 9.68	+18.76	43° 4.5'
14.64	+6.50	+4.24	-15.00	- 9.67	+20.42	42° 50'
16.40	+8.78	+5.72	-16.69	- 9.51	+24.02	42° 23'
18.33	+11.29	+7.34	-18.53	- 9.32	+27.96	41° 58'
20.45	+14.16	+9.21	-20.48	- 8.94	+32.32	41° 33'
22.77	+17.38	+11.30	-22.58	- 8.44	+37.12	41° 10'
25.31	+20.95	+13.63	-24.84	- 7.81	+42.40	40° 48'
31.03	+29.23	+19.03	-29.85	- 6.15	+54.42	40° 9'
34.25	+33.94	+22.10	-32.65	- 5.15	+61.20	39° 52'
41.42	+44.55	+29.05	-38.82	- 2.78	+76.39	39° 21'
45.36	+50.46	+32.92	-42.20	- 1.41	+84.79	39° 8'

Table 3a - Median Fiber Stresses at Corner of Shear Web, $r = \infty$

$\frac{Qa}{Eh^3}$	$\frac{\sigma'_x a^2}{Eh^2}$	$\frac{\sigma'_y a^2}{Eh^2}$	$\frac{\tau'_{xy} a^2}{Eh^2}$	$\frac{\sigma'_{max} a^2}{Eh^2}$	$\frac{\sigma'_{min} a^2}{Eh^2}$	α	Effective width Ratio
8.61	0	0	- 8.61	8.61	- 8.61	45°	1
8.82	.0004	.00	- 8.83	8.83	- 8.83	"	.998
9.30	.0009	.00	- 9.35	9.35	- 9.35	"	.994
10.01	.000	.00	-10.12	10.12	-10.12	"	.988
10.56	.001	.00	-10.73	10.73	-10.73	"	.984
11.01	-.003	.00	-11.23	11.23	-11.23	"	.980
12.00	-.008	-.01	-12.34	12.33	-12.35	"	.972
13.20	-.017	-.02	-13.68	13.66	-13.70	"	.964
14.02	-.025	-.03	-14.63	14.60	-14.66	"	.958
15.25	-.037	-.04	-16.16	16.12	-16.20	"	.949
16.55	-.050	-.05	-17.56	17.51	-17.61	"	.942
17.86	-.062	-.06	-19.06	19.00	-19.12	"	.936
20.67	-.099	-.10	-22.32	22.22	-22.42	"	.926
24.30	-.141	-.14	-26.59	26.45	-26.73	"	.913
28.04	-.207	-.21	-30.99	30.78	-31.20	"	.904
32.04	-.270	-.27	-35.72	35.45	-35.99	"	.897
36.60	-.341	-.34	-41.10	40.76	-41.44	"	.890
41.76	-.425	-.43	-47.20	46.77	-47.63	"	.883
47.22	-.512	-.51	-53.65	53.14	-54.16	"	.880
53.22	-.612	-.61	-60.75	60.14	-61.36	"	.876
59.82	-.726	-.73	-68.55	67.82	-69.28	"	.872
66.69	-.839	-.84	-76.70	75.86	-77.54	"	.869

Table 3b - Median Fiber Stresses at Corner of Shear Web, $r = 1/4$

$\frac{Qa}{Eh^3}$	$\frac{\sigma'_x a^2}{Eh^2}$	$\frac{\sigma'_y a^2}{Eh^2}$	$\frac{\tau'_{xy} a^2}{Eh^2}$	$\frac{\sigma'_{min} a^2}{Eh^2}$	$\frac{\sigma'_{max} a^2}{Eh^2}$	α	Effective width Ratio
8.61	0	0	- 8.61	- 8.61	+ 8.61	45°	1
8.73	- .01	- .04	- 8.74	- 8.77	+ 8.71	44° 57'	.998
9.10	- .06	- .18	- 9.16	- 9.28	+ 9.04	44° 49'	.993
9.61	- .13	- .37	- 9.75	-10.00	+ 9.49	44° 39'	.986
10.21	- .23	- .61	-10.44	-10.86	+10.01	44° 28'	.978
10.86	- .33	- .90	-11.20	-11.83	+10.59	44° 17'	.969
11.55	- .45	- 1.21	-12.03	-12.88	+11.20	44° 6'	.959
12.27	- .59	- 1.56	-12.91	-13.97	+11.86	43° 55'	.950
13.02	- .74	- 1.93	-13.84	-15.20	+12.51	43° 46'	.941
13.81	- .90	- 2.34	-14.82	-16.47	+13.21	43° 36'	.931
14.64	-1.08	- 2.79	-15.86	-17.82	+13.95	43° 27'	.922
16.40	-1.48	- 3.76	-18.11	-20.77	+15.52	43° 14'	.905
18.33	-1.93	- 4.90	-20.60	-24.07	+17.23	42° 56'	.889
20.45	-2.45	- 6.17	-23.35	-27.74	+19.11	42° 43'	.875
22.77	-3.04	- 7.60	-26.39	-31.81	+21.17	42° 32'	.862
25.31	-3.70	- 9.18	-29.73	-36.30	+23.41	42° 22'	.851
31.03	-5.22	-12.82	-37.29	-46.51	+28.46	42° 5'	.832
34.25	-6.09	-14.88	-41.56	-52.28	+31.31	41° 59'	.824
41.42	-8.04	-19.50	-51.07	-64.62	+38.06	41° 47'	.810
45.36	-9.13	-22.06	-56.32	-72.29	+41.09	41° 43'	.805

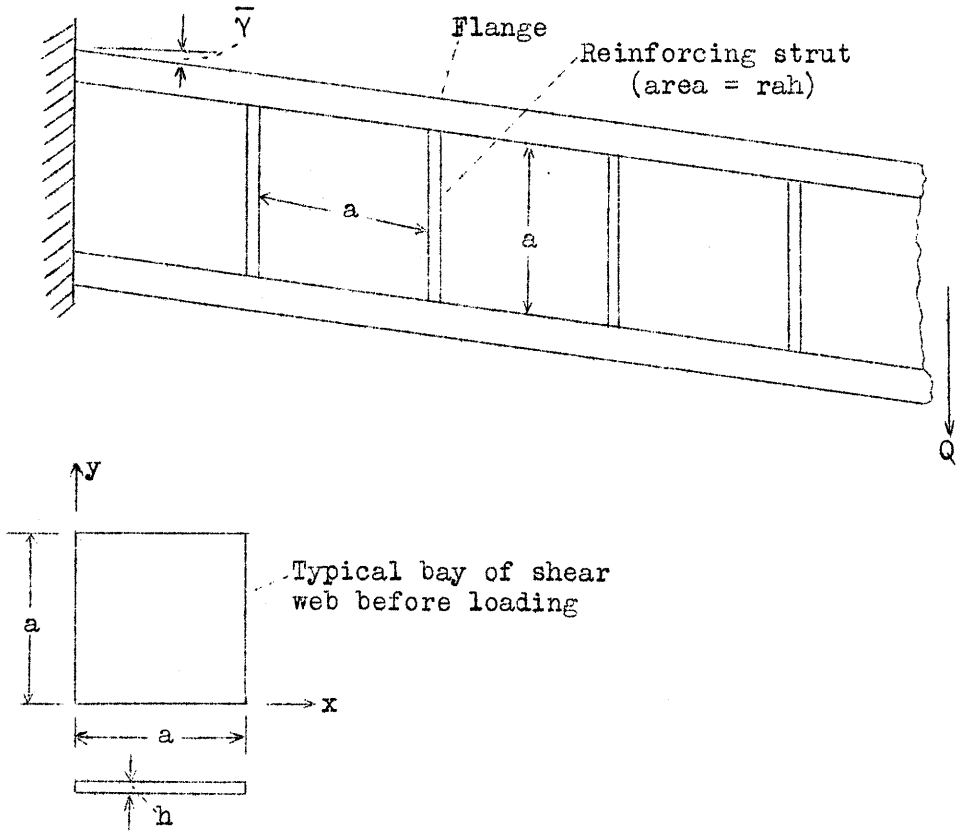

Figure 1.- Beam under shearing force Q and typical bay of shear web.

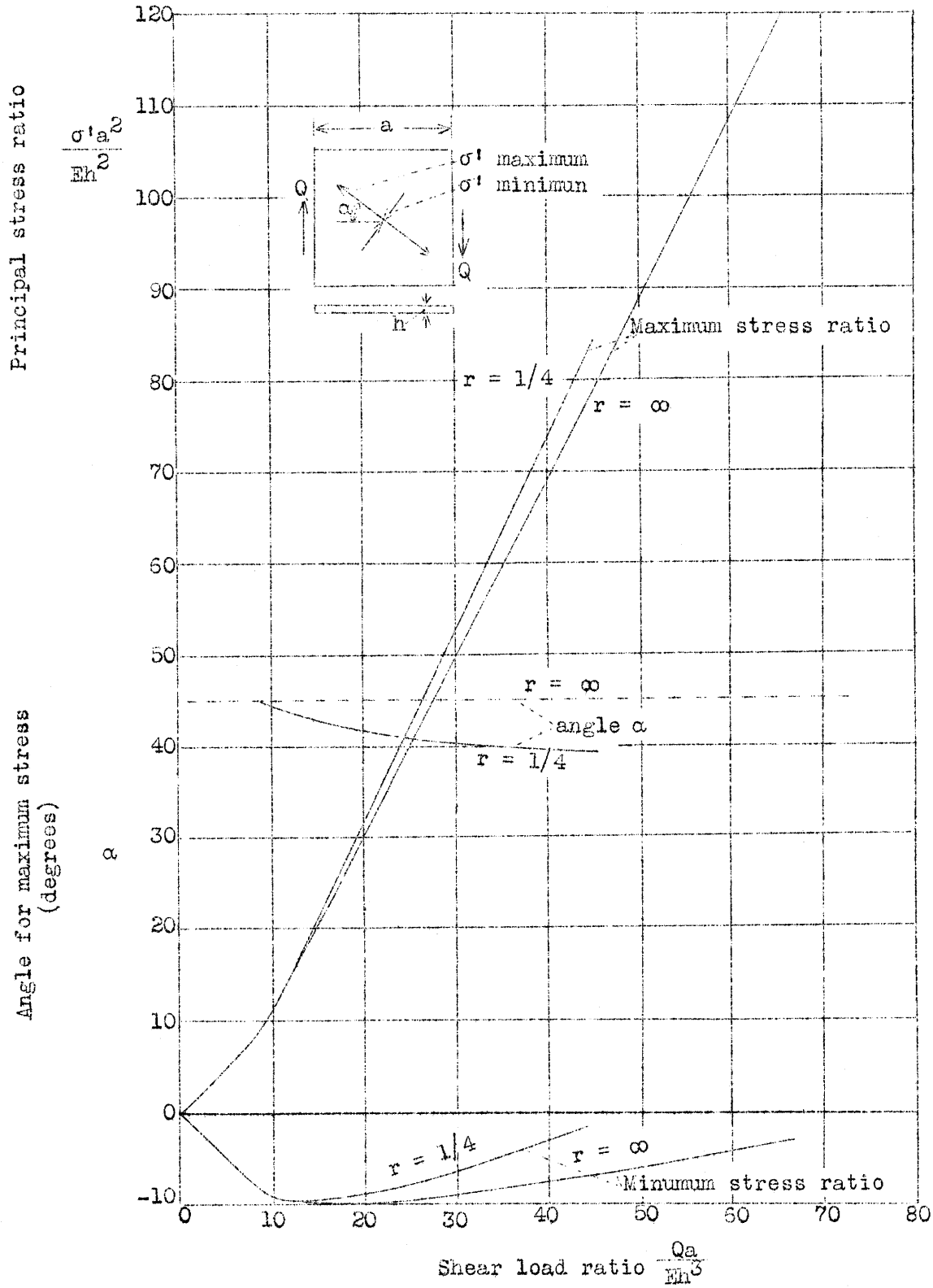

Figure 2.- Principal median fiber stresses and direction of maximum principal stress at center of shear bay. Ratio of strut area to sheet area r = 1/4, ∞.

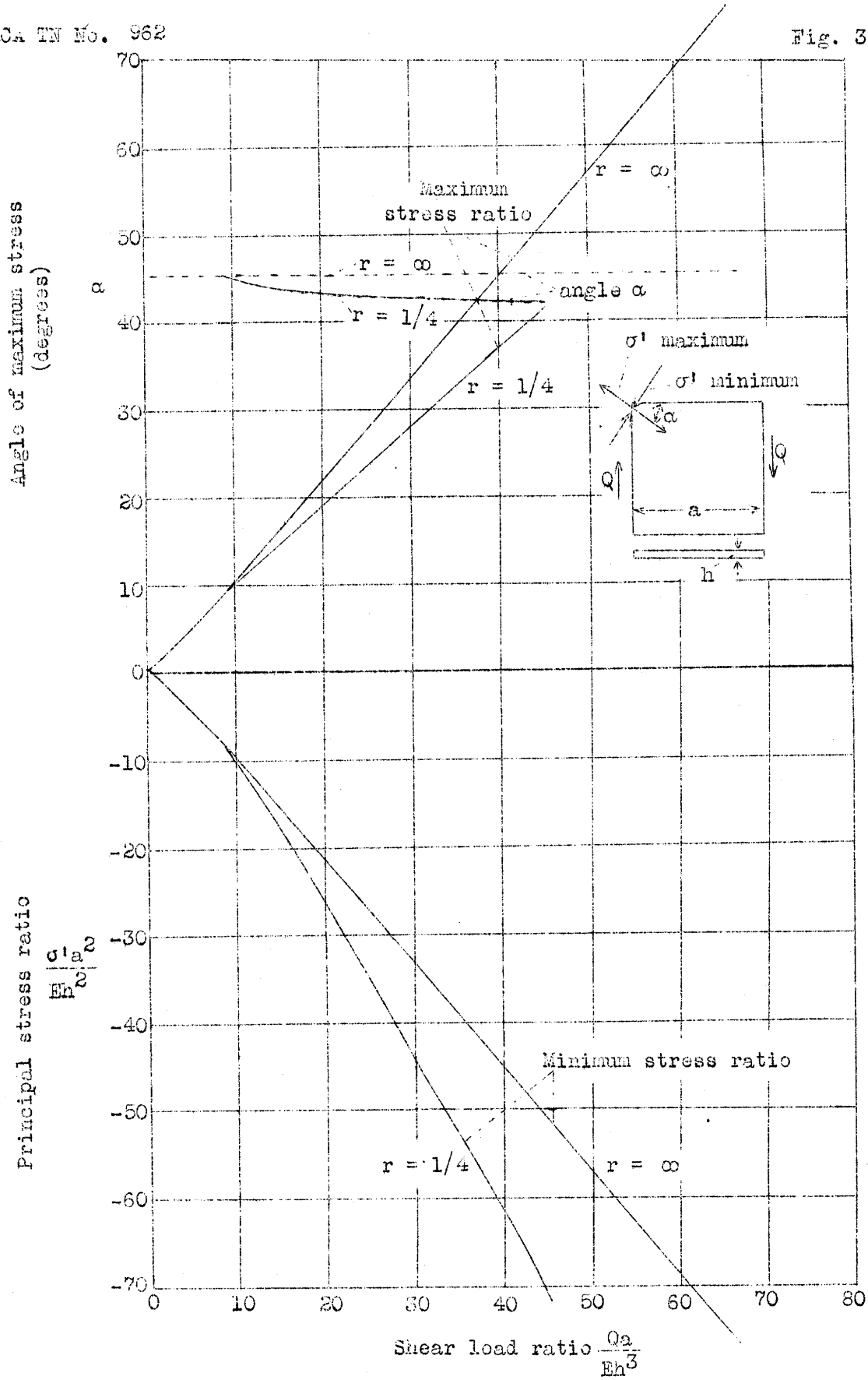

Figure 3.- Principal stresses and direction of maximum principal stress at corner of shear bay. Ratio of strut area to sheet area r=1/4, ∞.

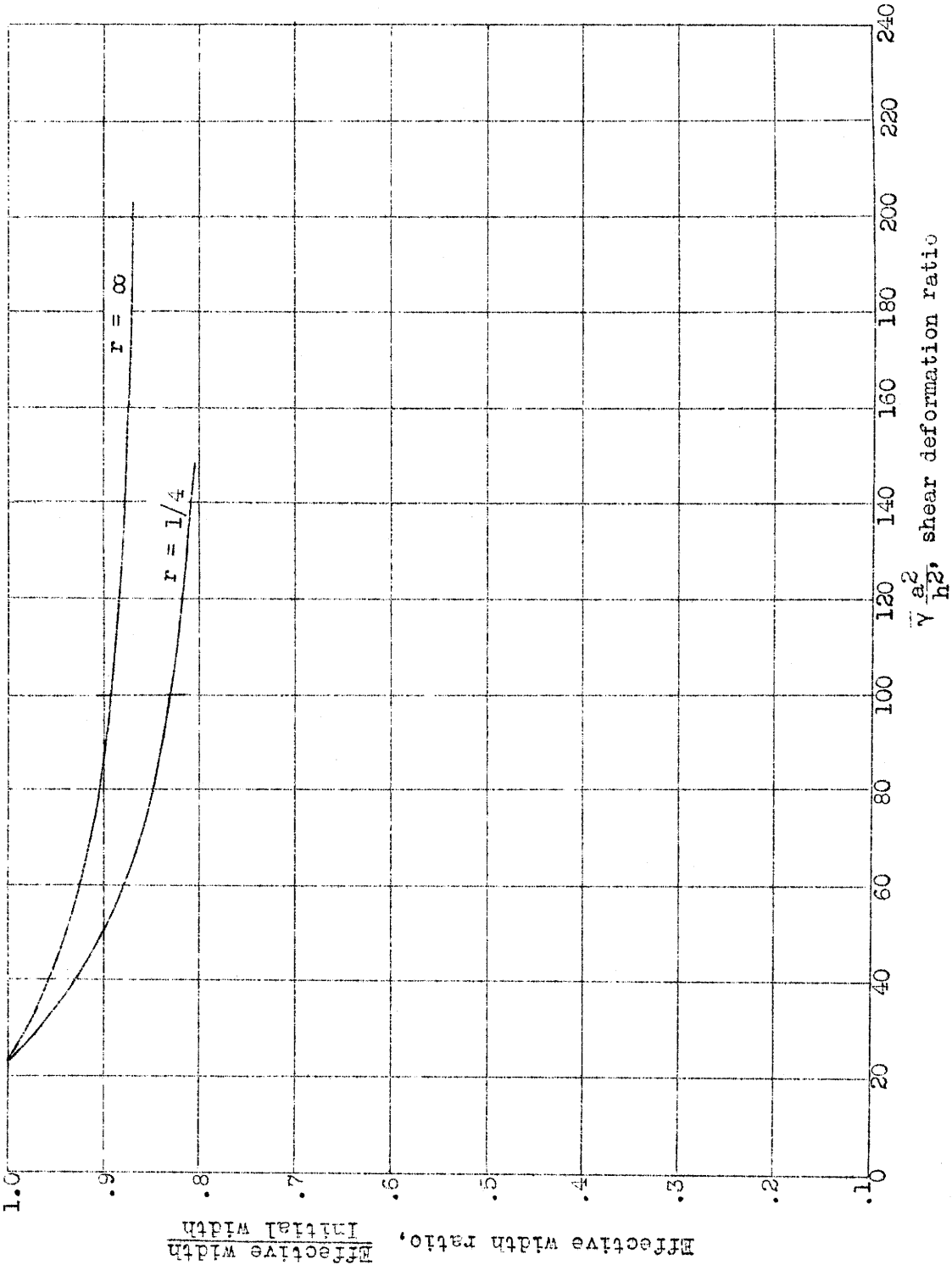

Figure 4.- Effective width of sheet in shear. Ratio of strut area to sheet area r = 1/4, ∞.

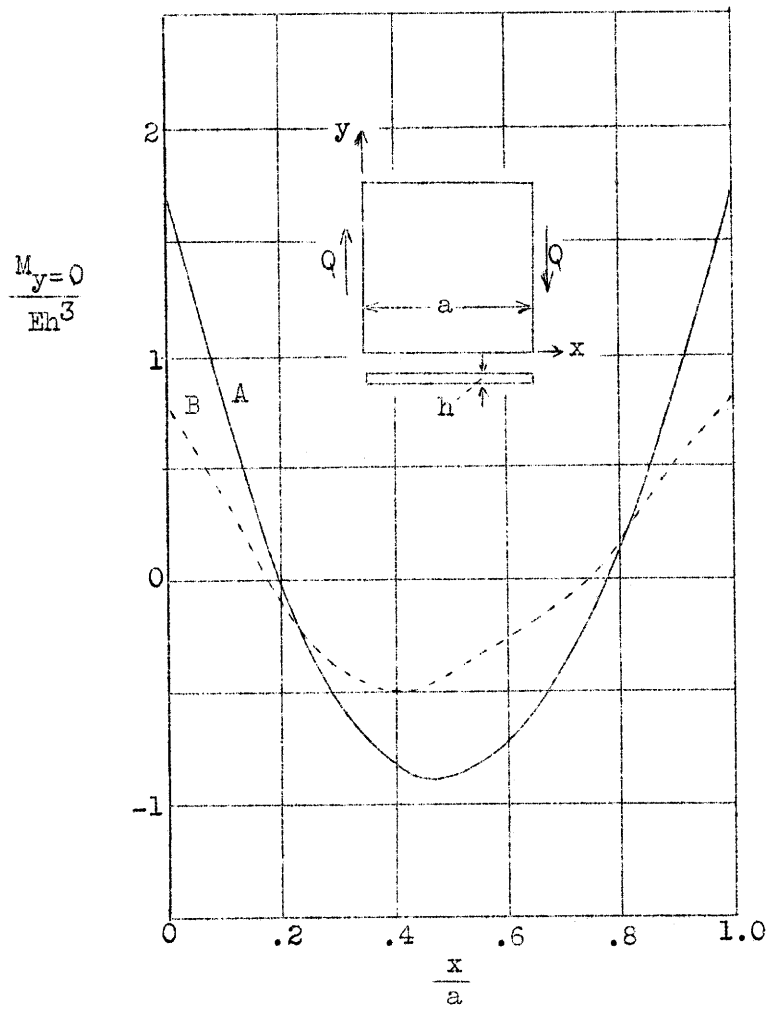

Figure 5.- Moment distribution in bottom flange (y = 0). Curve A, r = ∞, Q = 47.22 Eh^3/a, Curve B, r = 1/4, Q = 45.37 Eh^3/a.

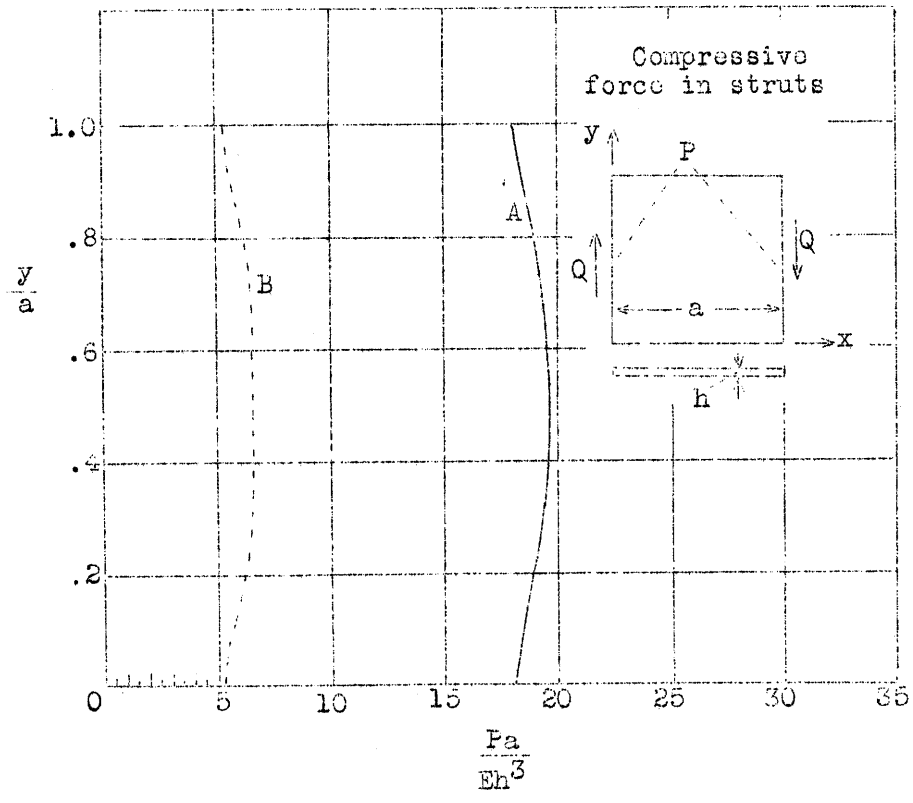

Figure 6.- Force distribution in struts at x = 0, a. Curve A, $r = \infty$, $Q = 47.22\ Eh^3/a$, Curve B, $r = 1/4$, $Q = 45.37\ Eh^3/a$, r = ratio of strut cross-sectional area to sheet cross-sectional area.

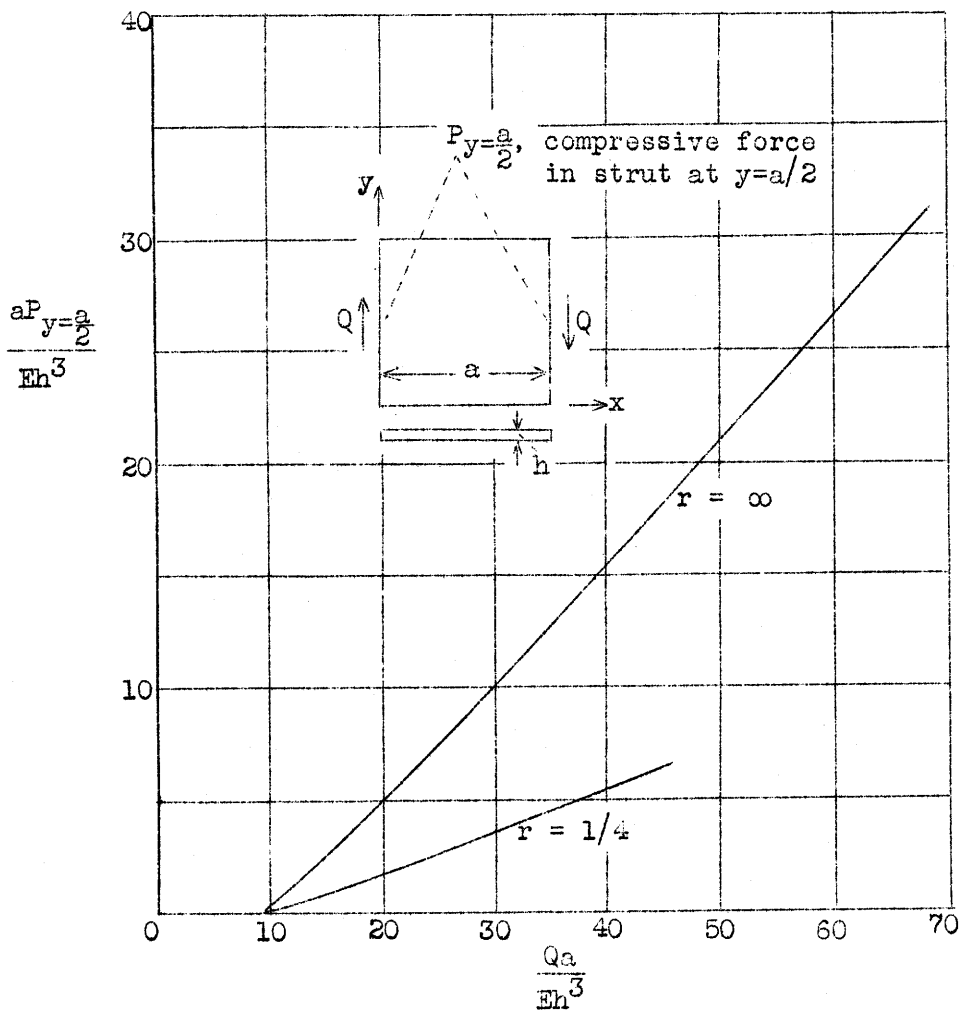

Figure 7.- Variation of maximum compressive force in strut $P_{y=a/2}$ with load. Ratio of strut area to sheet area $r = 1/4, \infty$.

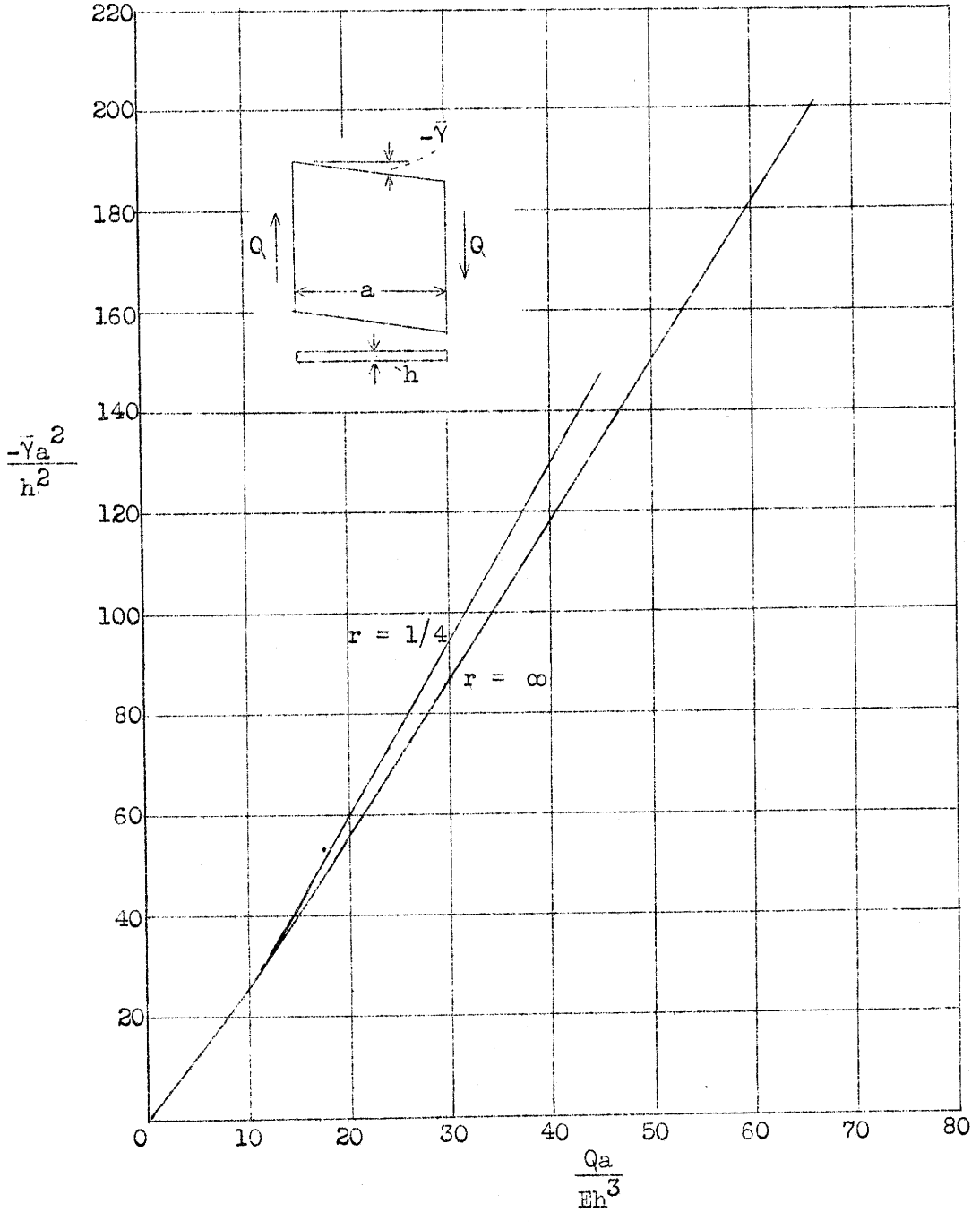

Figure 8.- Shear deformation of beam for ratio of strut area to web area r = 1/4, ∞.

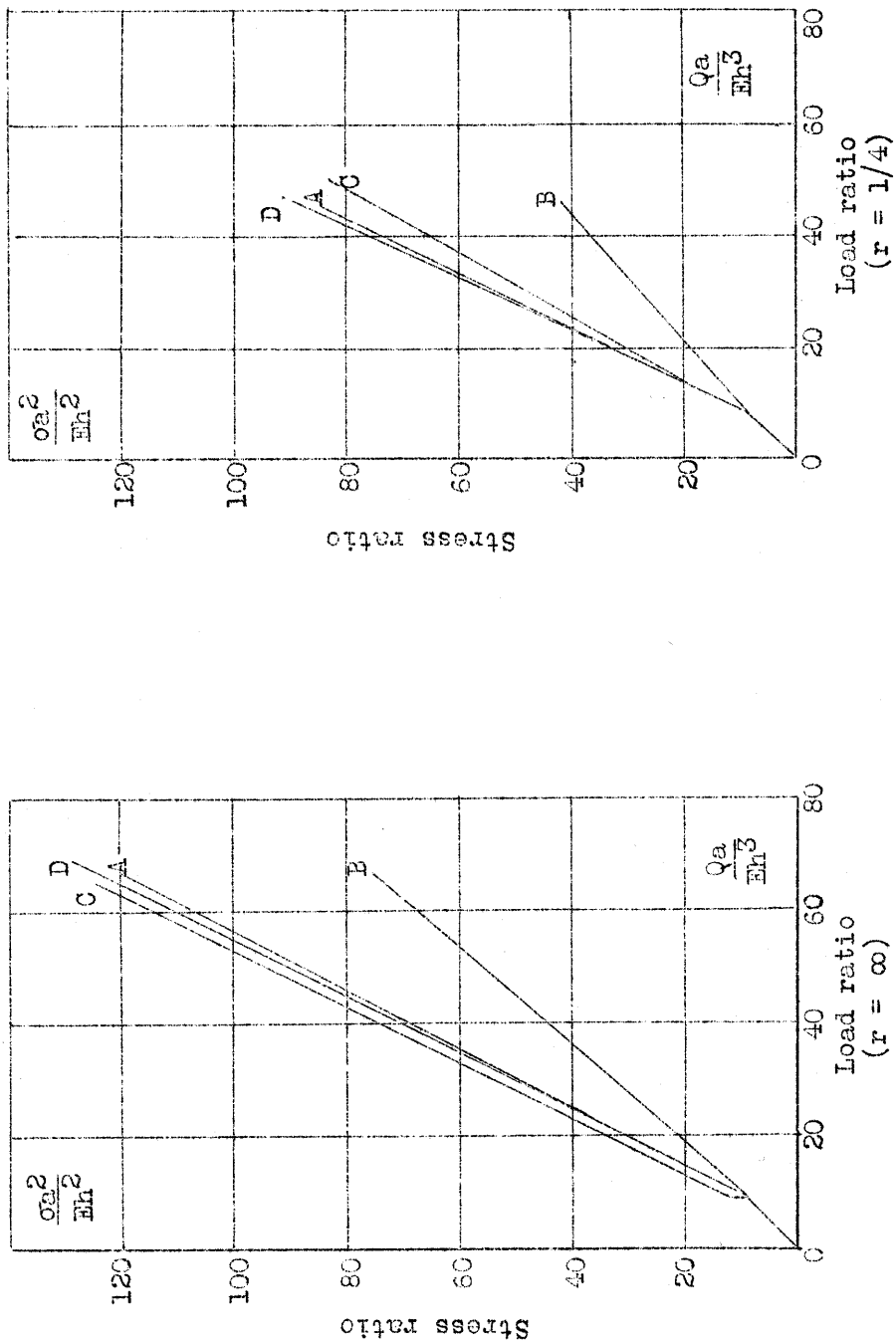

Figure 9.- Comparison of maximum median fiber stresses. σ, r = ratio of strut cross-sectional area to sheet cross-sectional area; curve A, center of plate, present paper; curve B, corner of plate, present paper; curve C, all points in plate, references 11 and 12; curve D, all points in plate, reference 13.

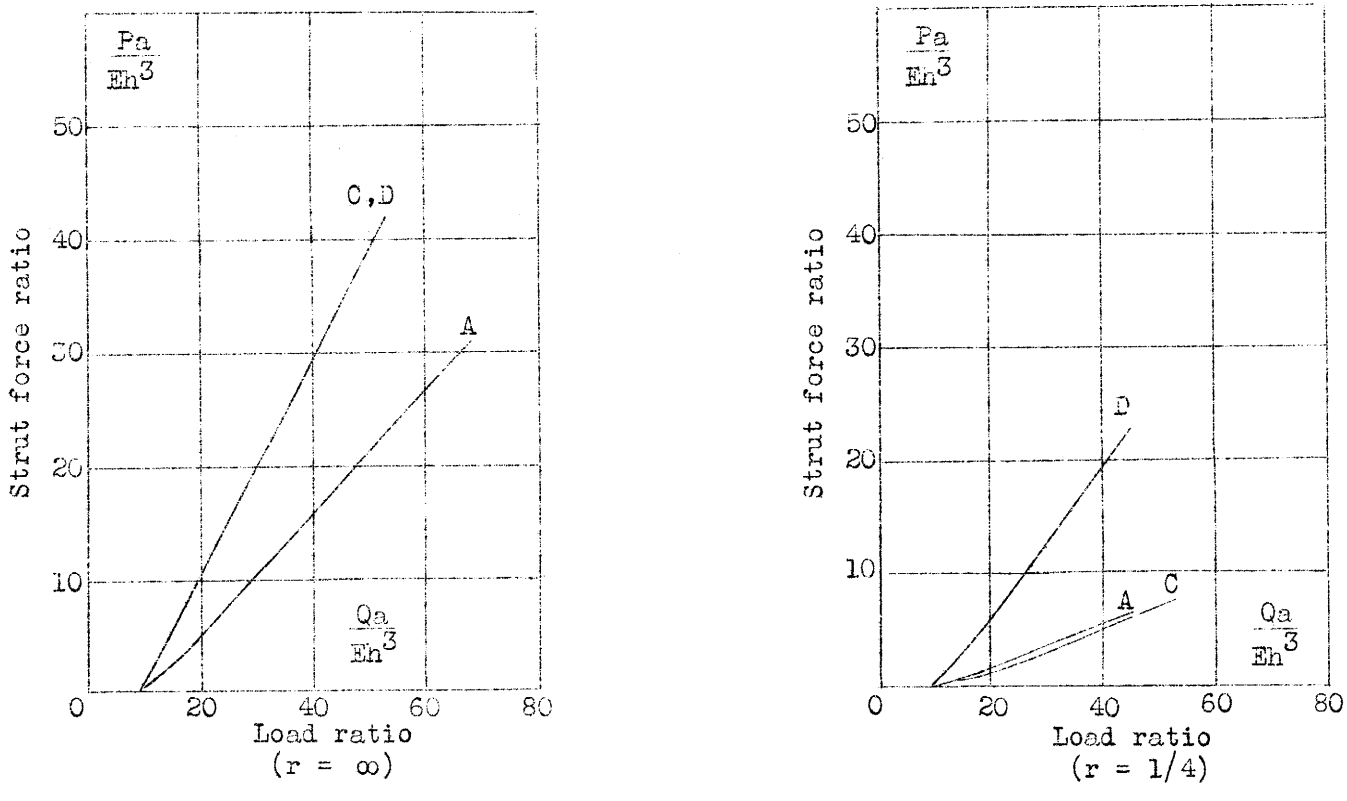

Figure 10.- Comparison of compressive force P in strut, r = ratio of strut cross-sectional area to sheet cross-sectional area; curve A, midpoint of strut, present paper; curve C, anywhere in strut, references 11 and 12; curve C, anywhere in strut, reference 13.

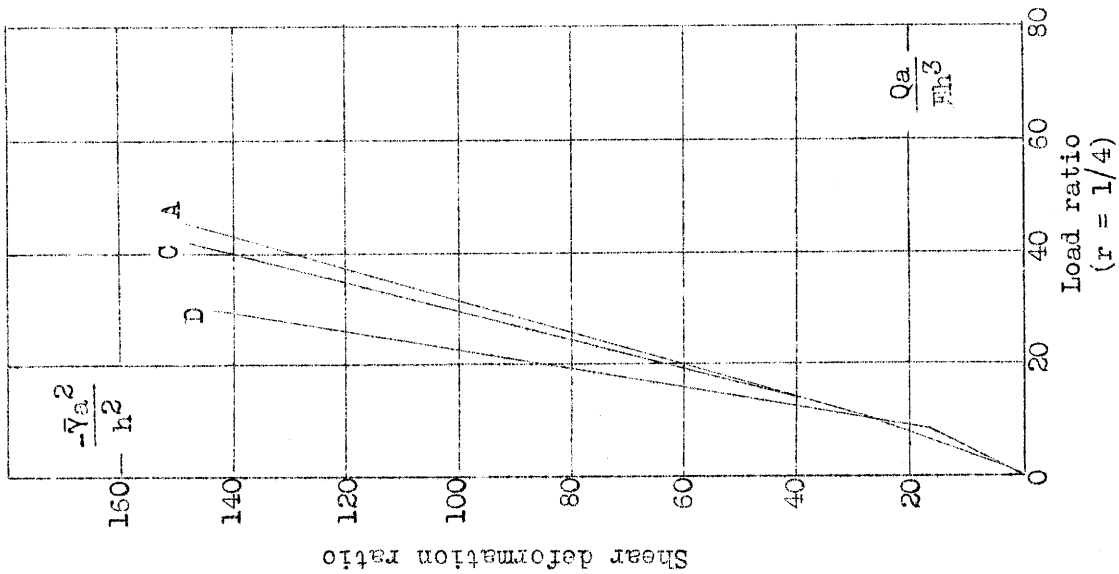

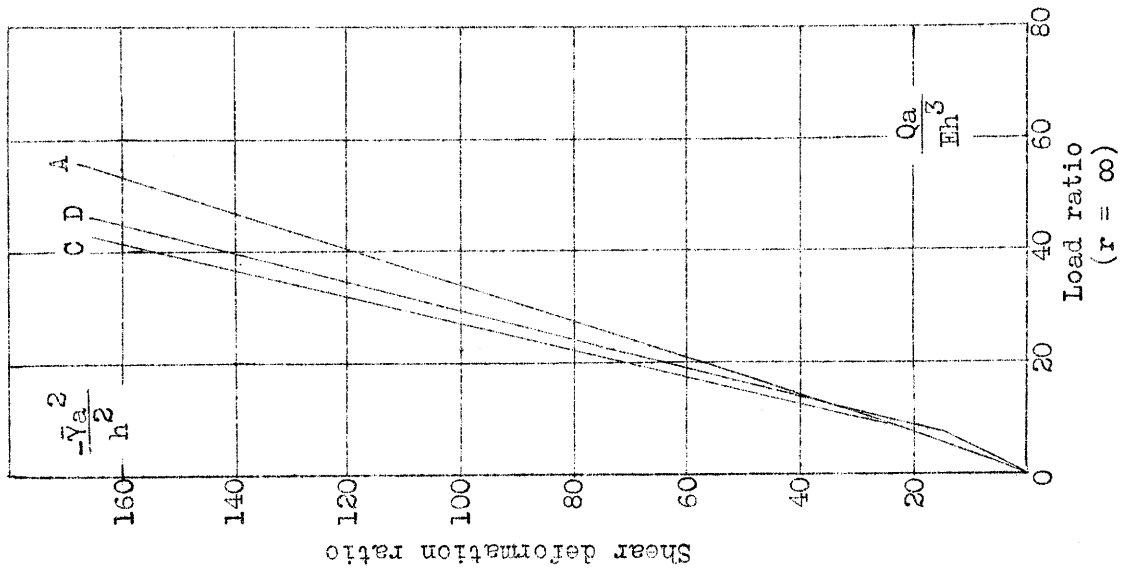

Figure 11.- Comparison of shear deformation $-\bar{\gamma}$, r = ratio of strut cross-sectional area to sheet cross-sectional area; curve A, present paper; curve C, references 11 and 12; curve D, reference 13.